

2003

Chemical composition of Asian continental outflow over the western Pacific: Results from Transport and Chemical Evolution over the Pacific (TRACE-P)

R. S. Russo

R. W. Talbot

See next page for additional authors

Follow this and additional works at: <https://digitalcommons.uri.edu/gsofacpubs>

Terms of Use

All rights reserved under copyright.

Citation/Publisher Attribution

Russo, R., et al. (2003), Chemical composition of Asian continental outflow over the western Pacific: Results from Transport and Chemical Evolution over the Pacific (TRACE-P), *J. Geophys. Res.*, 108, 8804, doi: 10.1029/2002JD003184, D20.
Available at: <https://doi.org/10.1029/2002JD003184>

This Article is brought to you for free and open access by the Graduate School of Oceanography at DigitalCommons@URI. It has been accepted for inclusion in Graduate School of Oceanography Faculty Publications by an authorized administrator of DigitalCommons@URI. For more information, please contact digitalcommons@etal.uri.edu.

Authors

R. S. Russo, R. W. Talbot, J. E. Dibb, E. Scheuer, G. Seid, C. E. Jordan, H. E. Fuelberg, G. W. Sachse, M. A. Avery, S. A. Vay, D. R. Blake, N. J. Blake, E. Atlas, A. Fried, S. T. Sandholm, D. Tan, H. B. Singh, J. Snow, and Brian G. Heikes

Chemical composition of Asian continental outflow over the western Pacific: Results from Transport and Chemical Evolution over the Pacific (TRACE-P)

R. S. Russo,¹ R. W. Talbot,¹ J. E. Dibb,¹ E. Scheuer,¹ G. Seid,¹ C. E. Jordan,³
H. E. Fuelberg,² G. W. Sachse,³ M. A. Avery,³ S. A. Vay,³ D. R. Blake,⁴ N. J. Blake,⁴
E. Atlas,⁵ A. Fried,⁵ S. T. Sandholm,⁶ D. Tan,⁶ H. B. Singh,⁷ J. Snow,⁸ and B. G. Heikes⁸

Received 18 November 2002; revised 28 April 2003; accepted 13 May 2003; published 23 September 2003.

[1] We characterize the chemical composition of Asian continental outflow observed during the NASA Transport and Chemical Evolution over the Pacific (TRACE-P) mission during February–April 2001 in the western Pacific using data collected on the NASA DC-8 aircraft. A significant anthropogenic impact was present in the free troposphere and as far east as 150°E longitude reflecting rapid uplift and transport of continental emissions. Five-day backward trajectories were utilized to identify five principal Asian source regions of outflow: central, coastal, north-northwest (NNW), southeast (SE), and west-southwest (WSW). The maximum mixing ratios for several species, such as CO, C₂Cl₄, CH₃Cl, and hydrocarbons, were more than a factor of 2 larger in the boundary layer of the central and coastal regions due to industrial activity in East Asia. CO was well correlated with C₂H₂, C₂H₆, C₂Cl₄, and CH₃Cl at low altitudes in these two regions ($r^2 \sim 0.77$ – 0.97). The NNW, WSW, and SE regions were impacted by anthropogenic sources above the boundary layer presumably due to the longer transport distances of air masses to the western Pacific. Frontal and convective lifting of continental emissions was most likely responsible for the high altitude outflow in these three regions. Photochemical processing was influential in each source region resulting in enhanced mixing ratios of O₃, PAN, HNO₃, H₂O₂, and CH₃OOH. The air masses encountered in all five regions were composed of a complex mixture of photochemically aged air with more recent emissions mixed into the outflow as indicated by enhanced hydrocarbon ratios (C₂H₂/CO ≥ 3 and C₃H₈/C₂H₆ ≥ 0.2). Combustion, industrial activities, and the burning of biofuels and biomass all contributed to the chemical composition of air masses from each source region as demonstrated by the use of C₂H₂, C₂Cl₄, and CH₃Cl as atmospheric tracers. Mixing ratios of O₃, CO, C₂H₂, C₂H₆, SO₂, and C₂Cl₄ were compared for the TRACE-P and PEM-West B missions. In the more northern regions, O₃, CO, and SO₂ were higher at low altitudes during TRACE-P. In general, mixing ratios were fairly similar between the two missions in the southern regions. A comparison between CO/CO₂, CO/CH₄, C₂H₆/C₃H₈, NO_x/SO₂, and NO_y/(SO₂ + nss-SO₄) ratios for the five source regions and for the 2000 Asian emissions summary showed very close agreement indicating that Asian emissions were well represented by the TRACE-P data and the emissions

inventory. **INDEX TERMS:** 0365 Atmospheric Composition and Structure: Troposphere—composition and chemistry; 0368 Atmospheric Composition and Structure: Troposphere—constituent transport and chemistry; 0345 Atmospheric Composition and Structure: Pollution—urban and regional (0305)

Citation: Russo, R., et al., Chemical composition of Asian continental outflow over the western Pacific: Results from Transport and Chemical Evolution over the Pacific (TRACE-P), *J. Geophys. Res.*, 108(D20), 8804, doi:10.1029/2002JD003184, 2003.

¹University of New Hampshire, Durham, New Hampshire, USA.

²Florida State University, Tallahassee, Florida, USA.

³NASA Langley Research Center, Hampton, Virginia, USA.

⁴University of California, Irvine, Irvine, California, USA.

⁵National Center for Atmospheric Research, Boulder, Colorado, USA.

⁶Georgia Institute of Technology, Atlanta, Georgia, USA.

⁷NASA Ames Research Center, Moffett Field, California, USA.

⁸University of Rhode Island, Narragansett, Rhode Island, USA.

1. Introduction

[2] The impact of industrialization and population growth in Asia on the composition of the western Pacific troposphere over the last several decades was not well documented, but it is likely to have been very significant. Recently, Asian anthropogenic emissions have been increasing, and for some species, such as SO₂ and NO_x, they are projected to continue increasing over the next 20 years [Streets and Waldhoff, 2000; van Aardenne et al., 1999]. By

2020, China is predicted to be the largest emitter of NO_x in the world [van Aardenne *et al.*, 1999]. However, Streets *et al.* [2003] revealed that the economic downturn in Asia in the late 1990s resulted in lower SO_2 and NO_x emissions than expected. Owing to the potential of Asian emissions to modify the global tropospheric composition, it is crucial to the global community and to the formation of environmental policies to characterize and document these temporal variations in Asian emissions.

[3] It is well documented that Asian anthropogenic emissions and dust are transported over the North Pacific Ocean [e.g., Duce *et al.*, 1980; Merrill *et al.*, 1989; Jaffe *et al.*, 1999]. Several studies have documented the influence of Asian outflow on the western U. S. and the impact of rising Asian emissions on the global troposphere [e.g., Bernsten *et al.*, 1999; Jacob *et al.*, 1999; Yienger *et al.*, 2000]. The magnitude of this impact varies throughout the year due to different meteorological situations in the various seasons. During the summer and fall, the Pacific high is located over the western Pacific and inhibits outflow from the Asian continent. The high causes an easterly flow of aged marine air to the western Pacific. In the spring, this high-pressure system is displaced eastward allowing the rapid and direct transport of continental outflow from Asia to the western Pacific [Bachmeier *et al.*, 1996]. A strong Siberian high-pressure system is also present during winter [Fuelberg *et al.*, 2003]. These two high-pressure systems result in maximum outflow from the Asian continent occurring in the late winter and spring [Merrill *et al.*, 1989, 1997].

[4] Two previous aircraft missions were conducted to document the impact of seasonal variations in Asian outflow on the western Pacific. The Pacific Exploratory Mission (PEM)-West A was conducted in September–October 1991, and PEM-West B occurred in February–March 1994. Asian outflow was found to be the main contributor to the tropospheric composition below 5 km [Talbot *et al.*, 1997; Gregory *et al.*, 1997]. PEM-West B was characterized by two-fold enhancements in anthropogenic species, such as C_2H_2 , C_2H_6 , and C_3H_8 , and decreased photochemical activity compared to PEM-West A. Increased source emissions and the winter/spring time period of PEM-West B were the presumed explanations for these differences. Wet convection was an important mechanism for transporting air to the upper troposphere during both missions [Talbot *et al.*, 1997]. The PEM-West missions provided valuable documentation of the trace gas and aerosol signatures of Asian outflow and information about the impact of Asian emissions on the western Pacific troposphere.

[5] A wide variety of pollution sources contribute emissions to the western Pacific troposphere because of differences in demographic and industrialization patterns. This results in specific sources being more predominant in certain regions of Asia. Fossil fuel combustion (e.g., electrical power generation) is the primary source of energy in Asia leading to emissions of SO_2 , CO, CO_2 , hydrocarbons, and reactive nitrogen species. China is the largest Asian source of SO_2 because of its use of high sulfur coal as a primary energy source [Streets *et al.*, 2003; Carmichael *et al.*, 2003b; Kato and Akimoto, 1992]. Biofuels (e.g., crop residues, fuel wood, animal waste, and charcoal) are estimated to be $\sim 24\%$ of the total energy use [Streets and Waldhoff, 1998]. Biofuels are typically used for cooking and

heating and are the dominant energy source in developing countries. Also, biomass burning is widespread in southeast Asia [Crutzen and Andreae, 1990]. As a result, emissions of CO, hydrocarbons, CH_3Cl , and nitrogen species are expected from SE Asia. The domestic sector of central China is an important source of both fossil fuel and biofuel emissions [Carmichael *et al.*, 2003b]. Industrial activities (i.e., petroleum refining, solvent usage, fuel evaporation during storage and transport, and natural gas leakage) have a considerable impact on the tropospheric composition of East Asia and result in emissions of C_2Cl_4 , CCl_4 , CH_3CCl_3 , and CFCs [Blake *et al.*, 1996]. Also, biogenic (i.e., vegetation, ocean) emission and uptake processes influence the composition of the western Pacific [e.g., Talbot *et al.*, 1996a, 1997].

[6] The focus of the NASA TRACE-P mission was to provide a comprehensive assessment of the impact of these various pollution sources on the atmospheric composition of the western Pacific and to study the chemical evolution and aging of Asian outflow. A secondary goal of TRACE-P was to determine if increasing Asian emissions over the past decade had a measurable impact on the tropospheric chemistry over the western Pacific and if the emission projections were substantially correct. A variety of methods were used to analyze and study the TRACE-P data, including examining the partitioning of specific species, models, emission inventories, meteorology patterns, transport mechanisms, and air mass trajectories. The results are presented in the many companion papers in this issue. In this paper we characterize and compare the chemical composition of outflow originating from the predominant source regions identified on the Asian continent and its transport to the western Pacific.

2. Experiment

[7] The TRACE-P mission was conducted during February–April 2001. The scientific rationale for the mission, species measurement details, and descriptions of the individual flights are presented in the TRACE-P overview paper [Jacob *et al.*, 2003]. The large-scale meteorology of the region during February–April 2001 and air mass trajectory details are described by Fuelberg *et al.* [2003]. The measurements used in this paper were made on the NASA Dryden DC-8 aircraft. The mission was composed of 17 transit and science intensive flights in the geographic region of $0\text{--}50^\circ\text{N}$ latitude and $110\text{--}180^\circ\text{E}$ longitude. The aircraft flew at altitudes ranging from 0.3 to 12.5 km. Flight 6 was a transit flight from Guam to Hong Kong, Flights 7–12 were based out of Hong Kong, and Flights 13–17 were based out of Yokota Air Force Base, Japan.

3. Database

[8] The data utilized in this paper was collected during Flights 6–17 within the geographic region of $10\text{--}45^\circ\text{N}$ latitude and $110\text{--}150^\circ\text{E}$ longitude. Merged data products for specific time intervals were created by NASA Langley Research Center due to the wide range of measurement time resolutions for the various species. The data presented in this paper was averaged to a 1 min time resolution. Measurements reported as below the limit of detection of

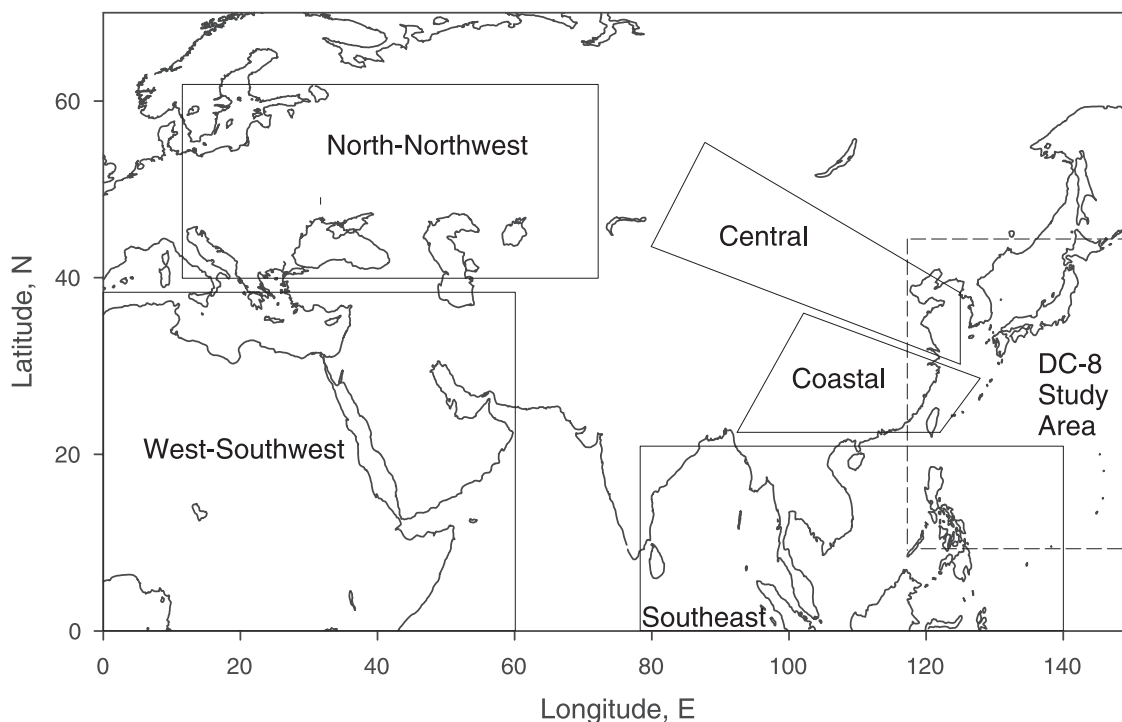


Figure 1. General locations of the five source regions of Asian continental outflow determined from 5-day backward trajectories. Data was collected within the geographic region 10–45°N and 110–150°E indicated by the dashed line box. This region only represents the DC-8 study area for Flights 6–17.

the instrument or that were influenced by stratospheric air were not included in the analysis. Stratospherically influenced air was defined as O_3 above 100 ppbv and CO less than ~ 70 ppbv (Northern Hemispheric background mixing ratio). When enhancements of both species were observed, the data was not removed from the database and was considered to be a mix of stratospheric and polluted air.

[9] Five-day backward trajectories, calculated by Florida State University [Fuelberg *et al.*, 2003], were used to identify continental source regions of outflow. Only measurements made during constant altitude flight legs were separated into the source region designations while data collected during the spiral ascents and descents was not included due to spatial heterogeneity in the air masses. Transport was dominated by strong westerly flow off of the Asian continent. Trajectories that did not travel over a continent, which was an infrequent occurrence, were not included in any of the source region groups.

[10] Examination of the five-day backward trajectories indicated that there were five general source regions of outflow (Figure 1). The five regions and their approximate latitude and longitude ranges are: central (30–60°N, 80–130°E), coastal (20–40°N, 90–130°E), southeast (SE) (0–25°N, 80–140°E), north-northwest (NNW) (40–65°N, 10–70°E), and west-southwest (WSW) (0–40°N, 0–60°E). These five source regions represent the general positions of the air masses five days prior to when they were encountered by the DC-8 over the western Pacific. Classification of the trajectories was based on their region of origin and the path that they followed to the western Pacific. Jordan *et al.* [2003] used the same source region classification to characterize the aerosol distribution in East

Asia and included examples and descriptions of the trajectories in each source region. Jordan *et al.* [2003] refers to the central region as “Channel.”

[11] The data was further separated into three altitude ranges, <2 km, 2–7 km, and >7 km, representing the boundary layer, middle troposphere, and upper troposphere. The three bins reflect the aircraft’s altitude at the sampling time. The ranges were chosen based on vertical distributions of O_3 and aerosols obtained by the DIAL instrument [Browell *et al.*, 2003]. The data was not evenly distributed across the five source regions during the time period of the measurements due to the altitudes flown by the DC-8. For example, the WSW region did not contain any boundary layer data, and the coastal region does not have data above ~ 4 km. Also, the trajectories that comprise the central region were constrained by mountains to the north and the Tibetan Plateau to the south. As a result, the central region does not have data >7 km because the high-altitude trajectories are not affected by the topography of this region [Jordan *et al.*, 2003].

4. Characterization of Flights 6–17

[12] This section discusses some general features of the observed trace gas distributions over the western Pacific for Flights 6–17, including measurements made during both constant altitude and spiral flight legs. The term “enhanced” is used to indicate when a species mixing ratio was greater than its Northern Hemisphere background mixing ratio. Measurements obtained during Flight 5, which was a transit flight from Hawaii to Guam, were used to estimate the background mixing ratios. Several

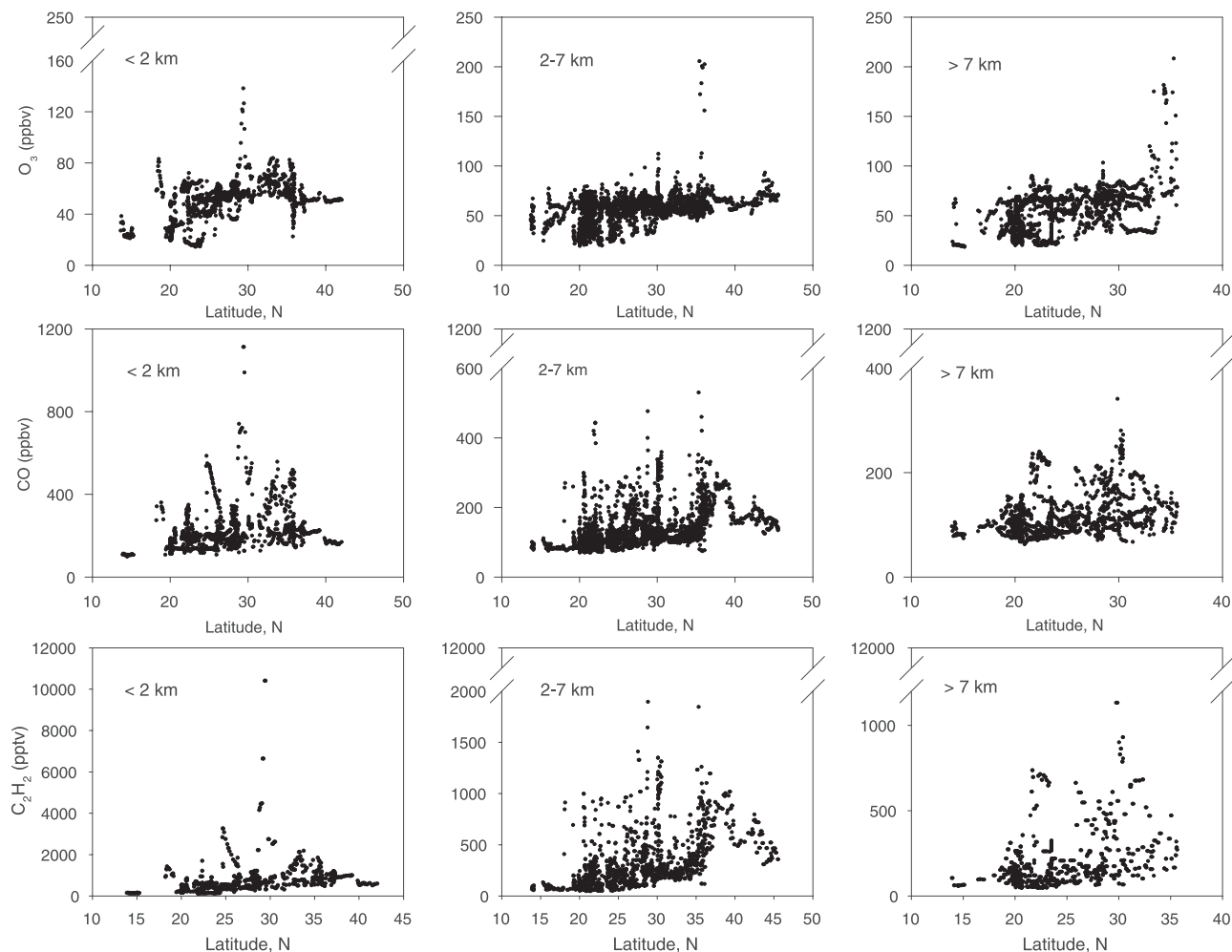


Figure 2. Latitudinal distribution of O_3 , CO , and C_2H_2 mixing ratios for Flights 6–17 for three altitude ranges: <2, 2–7, and >7 km.

of the back trajectories from Flight 5 only traveled over the ocean indicating that the air masses were composed of clean, aged marine air, and thus should be fairly representative of springtime, Northern Hemispheric background air. Background was considered to be the lowest one third of measurements in each altitude range. Background mixing ratios for several gases are listed below. The first value corresponds to the background mixing ratio below 2 km, the second corresponds to 2–7 km, and the third number is the background above 7 km: $\text{CO} = 90, 80, 74$ ppbv, $\text{O}_3 = 15, 20, 15$ ppbv, $\text{C}_2\text{Cl}_4 = 3, 2.5, 2$ pptv, $\text{CH}_3\text{Cl} = 530, 530, 520$ pptv, $\text{C}_2\text{H}_2 = 120, 65, 50$ pptv, $\text{C}_2\text{H}_6 = 650, 480, 420$ pptv, $\text{C}_3\text{H}_8 = 50, 20, 15$ pptv, and $\text{SO}_2 = 7, 20, 14$ pptv.

[13] The latitudinal distribution of O_3 in the three altitude ranges over the western Pacific basin was relatively similar. The mean O_3 mixing ratio at all altitudes was ~ 50 – 60 ppbv (Figure 2). The large peaks approaching 200 ppbv in the middle and upper altitudes occurred in air masses with a mix of stratospheric and polluted air. Coincident with the high O_3 were enhanced mixing ratios of CO (80–150 ppbv) indicative of a combustion influence in these air masses. As a result, the stratospheric influence could not be completely removed. The mean CO mixing ratio in the boundary layer

was ~ 200 ppbv, and 100–130 ppbv in the middle and upper troposphere (Figure 2). This suggests that an anthropogenic influence was present at all altitudes over the western Pacific. The abnormally large peak in the boundary layer near 30°N was due to the Shanghai plume which will be discussed in more detail in a later section.

[14] The most significant outflow occurred in the boundary layer between 20 and 40°N latitude, which corresponds to surface outflow directly off of China, Japan and Korea. Several species, such as CO , CO_2 , C_2H_2 , C_2H_6 , C_3H_8 , and C_2Cl_4 , exhibited enhanced mixing ratios between ~ 30 and 45°N suggesting a general trend increasing with latitude (Figure 2, only CO and C_2H_2 shown). This feature was particularly noticeable in the middle altitudes. Several companion papers also concluded that the strongest outflow occurred in this midlatitude band [e.g., Liu *et al.*, 2003; Vay *et al.*, 2003]. During PEM-West B, Blake *et al.* [1997] found a sharp transition at 25°N latitude with stronger outflow and larger mixing ratios for C_2H_6 , C_2H_2 , and C_2Cl_4 to the north, and this trend was most pronounced in the middle altitudes. Both the location of the major industrial areas and the strong outflow conditions in the late winter and spring at these latitudes were proposed to be responsible for the high mixing ratios.

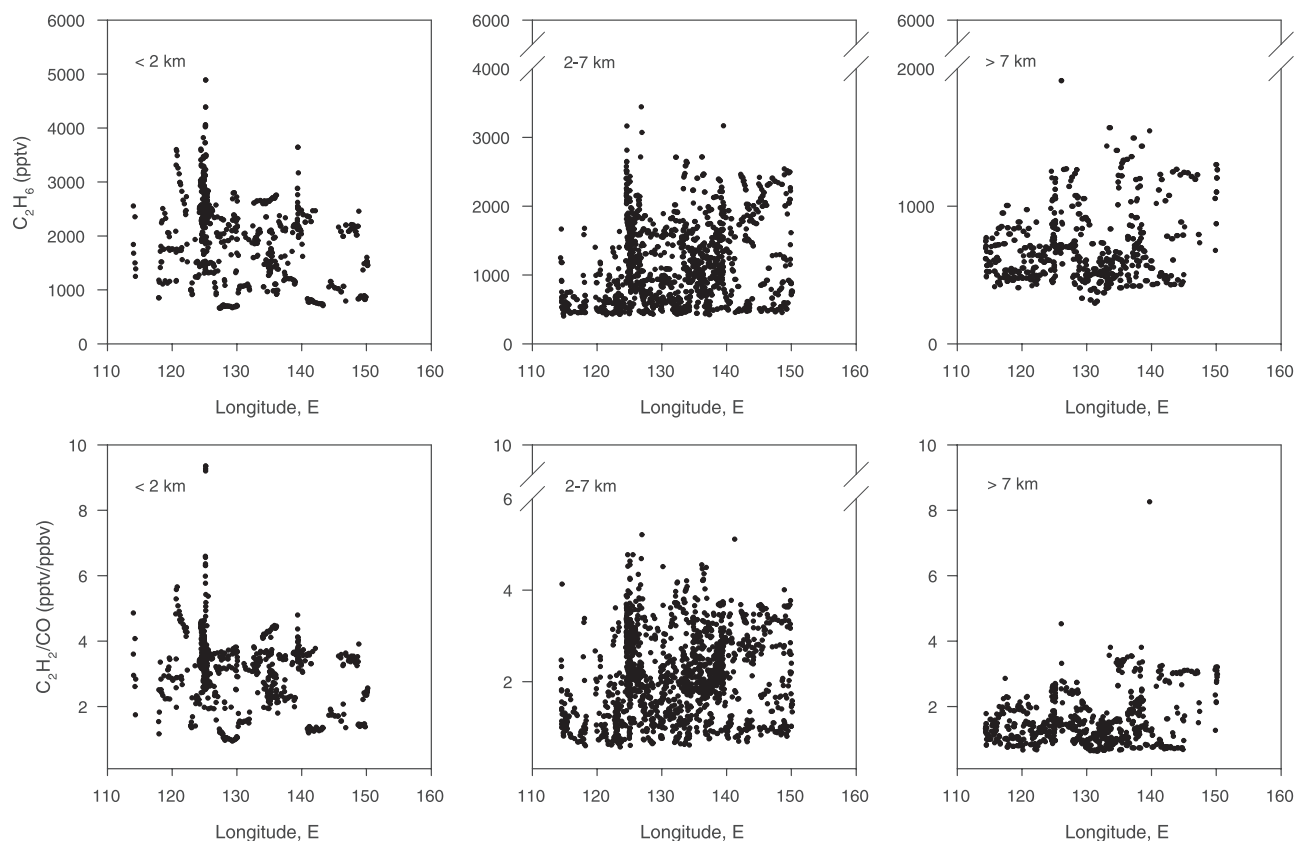


Figure 3. Longitudinal distribution of C_2H_6 mixing ratios and the C_2H_2/CO ratio for Flights 6–17 for <2, 2–7, and >7 km.

[15] An important finding of TRACE-P was that significant outflow was encountered in the middle and upper troposphere and as far east as $150^\circ E$ longitude (Figure 3). This indicates that anthropogenic influences were not confined to surface regions close to the Asian continent and suggests that emissions were rapidly uplifted and transported over the western Pacific. CO, CO_2 , SO_2 , C_2Cl_4 , CH_3Cl , and non-methane hydrocarbons (NMHCs), such as C_2H_2 , C_2H_6 , C_3H_8 , C_2H_4 , had enhanced mixing ratios in the free troposphere. For instance, at $150^\circ E$ longitude, CO reached over 250 ppbv in the middle altitudes and ~ 200 ppbv at higher altitudes. SO_2 mixing ratios peaked at approximately 6000 pptv in the middle altitude range. Also, C_2H_6 reached ~ 3000 pptv and ~ 1500 pptv in the middle and upper troposphere, respectively (Figure 3). In addition, Vay *et al.* [2003] found that the most efficient continental outflow and that nearly 80% of the CO_2 flux from the Asian continent occurred in the middle troposphere between 35 and $40^\circ N$.

[16] The relative age of an air mass resulting from atmospheric processing (mixing and photochemistry) can be estimated because of the different reactivities of chemical species emitted during combustion. NMHCs with short lifetimes will be removed from an air mass before longer-lived species; thus the mixing ratio of the short-lived species will decrease more quickly and alter the ratio value [e.g., McKeen and Liu, 1993; Smyth *et al.*, 1996]. The C_2H_2/CO and C_3H_8/C_2H_6 ratios are used in this paper to indicate air mass processing. A higher ratio (i.e., $C_2H_2/CO > 3$, $C_3H_8/C_2H_6 > 0.3$) suggests that an air mass contains recent emissions (less than a few days old) while a lower ratio

(i.e. $C_2H_2/CO < 1$, $C_3H_8/C_2H_6 < 0.1$) is indicative of an aged air mass (~ 1 week old) [e.g., Gregory *et al.*, 1997].

[17] During TRACE-P, both recent and aged emissions reached the free troposphere and were transported into the central Pacific as indicated by the longitudinal distribution of the C_2H_2/CO (Figure 3) and C_3H_8/C_2H_6 ratios. At $150^\circ E$ longitude, the C_2H_2/CO ratio had values as large as 4, and this was particularly noticeable in the middle altitude range. These results indicate that the combustion emissions were only 2 or 3 days old, implying rapid uplifting from the Asian continent and transport to these remote oceanic areas. The C_3H_8/C_2H_6 ratio demonstrated similar behavior and trends in its values. In each altitude range and at $150^\circ E$ longitude, the C_3H_8/C_2H_6 ratio reached values of approximately 0.2 and higher.

5. Characterization of Air Mass Source Regions

[18] This section discusses and compares the characteristics of the five principal Asian source regions identified by analysis of backward trajectories. Atmospheric tracer species were used to determine which pollution sources contributed emissions to regional outflow. Elevated mixing ratios of CO and C_2H_2 are indicative of combustion sources [Singh and Zimmerman, 1992]. C_2Cl_4 is an industrial/urban tracer since its only known source is through anthropogenic activities [Blake *et al.*, 1996; Wang *et al.*, 1995]. In addition, CH_3Cl and HCN are good tracers of biomass burning [Blake *et al.*, 1996; Singh *et al.*, 2003; Li *et al.*, 2003]. Tables 1–5 present summary statistical information describing the chemical

Table 1. Mixing Ratios for Selected Species From the Central Source Region^a

| Species | <2 km | | | | | | 2–7 km | | | | | |
|--------------------------------------------------------------|-------|--------|-----------|-------|------|-----|--------|--------|----------|------|------|-----|
| | Mean | Median | Std. Dev. | Max | Min | N | Mean | Median | Std.Dev. | Max | Min | N |
| O ₃ | 64 | 64 | 13 | 138 | 41 | 229 | 60 | 61 | 6 | 76 | 47 | 129 |
| CO | 303 | 264 | 153 | 1113 | 135 | 215 | 140 | 135 | 25 | 219 | 104 | 128 |
| NO | 73 | 48 | 77 | 399 | 0 | 211 | 14 | 11 | 11 | 64 | 2 | 82 |
| NO ₂ | 530 | 477 | 421 | 2926 | 8 | 184 | 55 | 51 | 38 | 177 | 0 | 71 |
| NO _y | 2430 | 1726 | 2249 | 13487 | 222 | 228 | 297 | 276 | 150 | 938 | 65 | 129 |
| HNO ₃ | 1323 | 833 | 1293 | 7412 | 222 | 229 | 202 | 169 | 110 | 938 | 106 | 120 |
| PAN | 1225 | 888 | 1014 | 4264 | 2 | 102 | 194 | 175 | 69 | 364 | 118 | 41 |
| SO ₂ | 4172 | 2621 | 4428 | 30736 | 353 | 205 | 80 | 65 | 64 | 284 | 10 | 91 |
| CO ₂ | 378 | 377 | 3 | 392 | 374 | 199 | 374 | 374 | 1 | 376 | 372 | 118 |
| H ₂ O ₂ | 567 | 446 | 441 | 2137 | 20 | 122 | 741 | 535 | 552 | 1725 | 134 | 49 |
| CH ₃ OOH | 98 | 88 | 50 | 293 | 36 | 107 | 228 | 225 | 108 | 482 | 104 | 35 |
| CH ₂ O | 2640 | 1690 | 2884 | 9824 | 208 | 35 | 85 | 82 | 19 | 122 | 61 | 17 |
| C ₂ H ₆ | 2695 | 2540 | 662 | 4888 | 1396 | 110 | 1415 | 1334 | 221 | 1968 | 1125 | 44 |
| C ₂ H ₄ | 396 | 106 | 681 | 3052 | 4 | 108 | 27 | 19 | 22 | 93 | 3 | 44 |
| C ₂ H ₂ | 1465 | 860 | 1639 | 10403 | 308 | 110 | 339 | 313 | 107 | 645 | 209 | 44 |
| C ₃ H ₈ | 1010 | 822 | 586 | 3774 | 271 | 110 | 308 | 279 | 96 | 540 | 184 | 44 |
| C ₆ H ₆ | 431 | 240 | 549 | 3101 | 61 | 110 | 64 | 62 | 25 | 147 | 28 | 44 |
| i-C ₄ H ₁₀ | 205 | 125 | 231 | 1345 | 31 | 110 | 40 | 39 | 16 | 83 | 15 | 44 |
| n-C ₄ H ₁₀ | 290 | 209 | 229 | 1384 | 46 | 110 | 67 | 58 | 30 | 151 | 27 | 44 |
| CH ₄ | 1856 | 1855 | 33 | 1983 | 1788 | 208 | 1797 | 1794 | 13 | 1837 | 1767 | 118 |
| C ₂ Cl ₄ | 18 | 12 | 19 | 123 | 8 | 110 | 6 | 6 | 2 | 10 | 4 | 44 |
| CCl ₄ | 104 | 100 | 11 | 162 | 98 | 110 | 99 | 99 | 1 | 102 | 97 | 44 |
| CH ₃ CCl ₃ | 43 | 41 | 5 | 66 | 40 | 110 | 40 | 40 | 0 | 41 | 39 | 44 |
| CH ₃ Cl | 654 | 559 | 239 | 1677 | 530 | 110 | 568 | 563 | 23 | 643 | 542 | 44 |
| CH ₃ Br | 10 | 9 | 4 | 29 | 8 | 110 | 9 | 9 | 0.27 | 9 | 8 | 44 |
| CFC-11 | 264 | 262 | 7 | 293 | 259 | 110 | 259 | 259 | 2 | 262 | 255 | 44 |
| CFC-12 | 543 | 540 | 12 | 615 | 534 | 110 | 535 | 535 | 3 | 543 | 528 | 44 |
| CFC-113 | 81 | 80 | 5 | 113 | 77 | 110 | 79 | 79 | 1 | 80 | 78 | 44 |
| C ₂ H ₂ /CO | 3.87 | 3.37 | 1.34 | 9.35 | 2.24 | 102 | 2.40 | 2.35 | 0.40 | 3.82 | 1.91 | 43 |
| C ₃ H ₈ /C ₂ H ₆ | 0.35 | 0.33 | 0.09 | 0.77 | 0.19 | 110 | 0.21 | 0.21 | 0.04 | 0.31 | 0.15 | 44 |

^aMixing ratios are given in parts per trillion by volume except for O₃, CO, and CH₄ which are in parts per billion by volume and for CO₂ which is in parts per million by volume. The C₂H₂/CO ratio is in parts per trillion by volume/parts per billion by volume.

composition of the five source regions. This information is used in our discussion of each of the five source regions.

5.1. Central

[19] The most striking feature of the central region was the Shanghai plume which was sampled in the boundary layer (~0.3 km) during Flight 13 over the Yellow Sea (Figure 4). Several species had their highest mixing ratios measured during the entire mission in this plume (Table 1), including CO, SO₂, C₂H₂, C₂H₆, C₂H₄, C₃H₈, CH₂O, C₂Cl₄, CCl₄, CH₃CCl₃, CH₃Cl, HNO₃, PAN, and NO_y (NO_y = NO + NO₂ + HNO₃ + PAN + PPN + C₁-C₅ alkyl nitrates). For example, CO mixing ratios peaked at ~1100 ppbv, C₂H₂ at ~10,000 pptv, SO₂ at ~31,000 pptv, C₂Cl₄ at 123 pptv, and CH₃Cl at ~1700 pptv. Aerosol Ca²⁺ and NO₃⁻ were also significantly enhanced in the boundary layer indicating a strong dust and anthropogenic influence [Jordan *et al.*, 2003]. The Shanghai plume was largely composed of recent combustion emissions that were less than 1 day old (maximum C₂H₂/CO = 9.4, C₃H₈/C₂H₆ = 0.77). The observed composition of the plume was most likely quite similar to its original composition. Photochemical species, such as O₃, PAN, HNO₃, CH₃OOH, and H₂O₂, were also enhanced. For example, O₃ reached ~140 ppbv while PAN peaked near 4300 pptv. These high levels indicate significant photochemical activity even at this time of the year. Correlations of O₃ and CO ($r^2 = 0.82$) and O₃ and PAN ($r^2 = 0.69$) were fairly robust and suggested that O₃ and PAN were photochemically produced from combustion derived precursor gases in the outflow. The strong correlation between O₃ and CO reflects

the recent emission inputs into the Shanghai plume where dilution and mixing processes had not acted to significantly alter the overall composition of the plume. O₃ and CO were poorly correlated in the other four source regions, where the emissions were clearly more than 1 day old. Simpson *et al.* [2003] discuss the chemistry and production of C₂-C₅ alkyl nitrates in Asian outflow and concluded that the Shanghai plume contained very fresh emissions of these species and that dilution was not a significant factor affecting the observed plume composition.

[20] Pollution plumes from other urban regions around the world show enhancements in many of the same anthropogenic species, specifically CO, NMHCs, and halocarbons. However, these enhancements occur in varying degrees compared to the Shanghai plume. For example, NMHC mixing ratios in the southeast U.S. and Houston, Texas have been found to be substantially higher than in the Shanghai plume [e.g., Kang *et al.*, 2001]. The mixing ratios of several hydrocarbons (e.g., C₂H₆, C₃H₈, C₂H₂, C₆H₆) have been found to be factors of ~2–50 higher in Mexico City [Blake and Rowland, 1995]. Also, C₂H₆, C₂H₂, C₃H₈, C₆H₆, and CO were observed to be approximately a factor of 2 larger in London in the winter than the maximum values of these species observed in the Shanghai plume [Derwent *et al.*, 1995]. A notable difference between the Shanghai plume and other urban regions is the large influence from biofuel emissions most likely reflecting their use for cooking and heating in East Asia. C₃H₈, C₂H₂, C₂H₆, C₆H₆, i-C₄H₁₀, and n-C₄H₁₀ mixing ratios observed in South Korea were fairly comparable with the Shanghai

Table 2. Mixing Ratios of Selected Species From the Coastal Source Region^a

| Species | <2 km | | | | | | 2–4 km | | | | | |
|--------------------------------------------------------------|-------|--------|-----------|------|------|-----|--------|--------|-----------|------|------|-----|
| | Mean | Median | Std. Dev. | Max | Min | N | Mean | Median | Std. Dev. | Max | Min | N |
| O ₃ | 41 | 43 | 14 | 83 | 15 | 290 | 58 | 60 | 6 | 69 | 43 | 111 |
| CO | 201 | 166 | 107 | 586 | 124 | 264 | 151 | 132 | 47 | 272 | 107 | 83 |
| NO | 7 | 2 | 15 | 79 | 0 | 221 | 23 | 17 | 20 | 110 | 5 | 94 |
| NO ₂ | 41 | 13 | 89 | 503 | 0 | 195 | 35 | 33 | 22 | 137 | 6 | 65 |
| NO _y | 541 | 386 | 525 | 3267 | 56 | 283 | 431 | 475 | 260 | 1096 | 24 | 110 |
| HNO ₃ | 439 | 322 | 365 | 2120 | 128 | 267 | 368 | 326 | 169 | 876 | 135 | 95 |
| PAN | 207 | 19 | 336 | 1065 | 1 | 104 | 142 | 115 | 126 | 412 | 15 | 51 |
| SO ₂ | 207 | 48 | 377 | 1554 | 4 | 105 | 27 | 21 | 19 | 120 | 10 | 38 |
| CO ₂ | 376 | 375 | 3.5 | 389 | 373 | 233 | 374 | 374 | 1.1 | 376 | 372 | 84 |
| H ₂ O ₂ | 1243 | 1176 | 611 | 3179 | 339 | 108 | 1404 | 1553 | 591 | 3093 | 416 | 58 |
| CH ₃ OOH | 470 | 351 | 359 | 1535 | 53 | 100 | 269 | 280 | 117 | 531 | 84 | 55 |
| CH ₂ O | 763 | 461 | 797 | 3553 | 92 | 90 | 265 | 245 | 128 | 488 | 55 | 32 |
| C ₂ H ₆ | 1498 | 1353 | 716 | 3598 | 669 | 105 | 1085 | 929 | 336 | 1974 | 793 | 39 |
| C ₂ H ₄ | 208 | 9 | 452 | 1794 | 3 | 93 | 30 | 22 | 25 | 87 | 3 | 23 |
| C ₂ H ₂ | 665 | 384 | 749 | 3264 | 125 | 105 | 376 | 255 | 222 | 908 | 181 | 39 |
| C ₃ H ₈ | 375 | 211 | 448 | 2069 | 27 | 105 | 171 | 131 | 89 | 375 | 65 | 39 |
| C ₆ H ₆ | 189 | 79 | 272 | 1207 | 30 | 105 | 77 | 42 | 55 | 185 | 27 | 39 |
| i-C ₄ H ₁₀ | 94 | 32 | 160 | 738 | 9 | 89 | 23 | 12 | 20 | 65 | 4 | 39 |
| n-C ₄ H ₁₀ | 121 | 38 | 211 | 1030 | 4 | 93 | 36 | 16 | 30 | 100 | 7 | 39 |
| CH ₄ | 1816 | 1808 | 34 | 1915 | 1735 | 241 | 1779 | 1776 | 11 | 1831 | 1761 | 72 |
| C ₂ Cl ₄ | 9 | 8 | 6 | 32 | 3 | 105 | 5 | 5 | 2 | 11 | 3 | 39 |
| CCl ₄ | 102 | 100 | 6 | 127 | 97 | 105 | 100 | 100 | 1 | 102 | 99 | 39 |
| CH ₃ CCl ₃ | 41 | 41 | 3 | 54 | 39 | 105 | 40 | 40 | 1 | 41 | 39 | 39 |
| CH ₃ Cl | 638 | 580 | 176 | 1333 | 522 | 105 | 589 | 575 | 32 | 662 | 549 | 39 |
| CH ₃ Br | 10 | 9 | 2 | 18 | 8 | 105 | 9 | 9 | 0.43 | 10 | 8 | 39 |
| CFC-11 | 262 | 261 | 4 | 277 | 256 | 105 | 261 | 261 | 1 | 264 | 259 | 39 |
| CFC-12 | 540 | 538 | 6 | 559 | 532 | 105 | 539 | 538 | 3 | 544 | 534 | 39 |
| CFC-113 | 80 | 80 | 1 | 85 | 77 | 105 | 80 | 80 | 1 | 81 | 79 | 39 |
| C ₂ H ₂ /CO | 2.46 | 2.28 | 1.19 | 5.66 | 0.94 | 94 | 2.27 | 1.91 | 0.71 | 3.94 | 1.66 | 31 |
| C ₃ H ₈ /C ₂ H ₆ | 0.19 | 0.16 | 0.12 | 0.58 | 0.04 | 105 | 0.15 | 0.13 | 0.05 | 0.24 | 0.08 | 39 |

^aMixing ratios are given in parts per trillion by volume except for O₃, CO, and CH₄ which are in parts per billion by volume and for CO₂ which is in parts per million by volume. The C₂H₂/CO ratio is in parts per trillion by volume/parts per billion by volume.

Table 3. Mixing Ratios of Selected Species From the SE Source Region^a

| Species | <2 km | | | | | | 2–7 km | | | | | | >7 km | | | | | |
|--------------------------------------------------------------|-------|--------|-----------|------|------|----|--------|--------|-----------|------|------|-----|-------|--------|-----------|------|------|-----|
| | Mean | Median | Std. Dev. | Max | Min | N | Mean | Median | Std. Dev. | Max | Min | N | Mean | Median | Std. Dev. | Max | Min | N |
| O ₃ | 39 | 40 | 3 | 43 | 27 | 25 | 52 | 57 | 13 | 72 | 27 | 244 | 39 | 32 | 17 | 70 | 18 | 620 |
| CO | 208 | 205 | 18 | 254 | 157 | 25 | 123 | 88 | 69 | 331 | 74 | 231 | 98 | 88 | 27 | 223 | 67 | 557 |
| NO | | | | | | | 16 | 15 | 12 | 130 | 1 | 171 | 92 | 47 | 157 | 805 | 9 | 377 |
| NO ₂ | | | | | | | 31 | 26 | 16 | 65 | 5 | 89 | 14 | 11 | 11 | 48 | 0 | 240 |
| NO _y | 795 | 796 | 43 | 884 | 730 | 25 | 369 | 301 | 325 | 1439 | 5 | 219 | 172 | 125 | 177 | 1158 | 6 | 589 |
| HNO ₃ | 784 | 783 | 47 | 884 | 713 | 25 | 336 | 238 | 230 | 1352 | 100 | 174 | 86 | 66 | 66 | 320 | 3 | 502 |
| PAN | 17 | 17 | 8 | 27 | 3 | 9 | 159 | 86 | 186 | 660 | 8 | 98 | 62 | 54 | 56 | 238 | 6 | 287 |
| SO ₂ | 23 | 20 | 11 | 45 | 7 | 16 | 32 | 23 | 56 | 415 | 6 | 102 | 38 | 21 | 51 | 284 | 10 | 93 |
| CO ₂ | 376 | 376 | 0.65 | 377 | 374 | 23 | 372 | 371 | 2 | 379 | 370 | 222 | 372 | 371 | 1 | 374 | 370 | 279 |
| H ₂ O ₂ | 5660 | 5699 | 508 | 6199 | 4857 | 9 | 739 | 266 | 1019 | 5391 | 48 | 96 | 164 | 109 | 154 | 686 | 15 | 210 |
| CH ₃ OOH | 1351 | 1331 | 223 | 1791 | 1121 | 10 | 257 | 216 | 195 | 1083 | 30 | 71 | 114 | 103 | 65 | 340 | 29 | 125 |
| CH ₂ O | 346 | 300 | 114 | 516 | 268 | 4 | 162 | 127 | 108 | 406 | 53 | 36 | 248 | 143 | 286 | 1138 | 56 | 50 |
| C ₂ H ₆ | 1182 | 1155 | 104 | 1412 | 1105 | 7 | 737 | 528 | 405 | 1775 | 422 | 88 | 594 | 514 | 194 | 1270 | 370 | 279 |
| C ₂ H ₄ | 6 | 6 | 1 | 8 | 5 | 5 | 31 | 14 | 38 | 132 | 2 | 43 | 16 | 5 | 31 | 160 | 3 | 84 |
| C ₂ H ₂ | 459 | 456 | 82 | 627 | 369 | 7 | 252 | 93 | 321 | 1210 | 48 | 88 | 129 | 89 | 105 | 609 | 47 | 279 |
| C ₃ H ₈ | 123 | 112 | 18 | 156 | 109 | 7 | 81 | 35 | 108 | 430 | 15 | 88 | 54 | 33 | 49 | 257 | 11 | 279 |
| C ₆ H ₆ | 88 | 86 | 16 | 118 | 70 | 7 | 53 | 13 | 84 | 328 | 3 | 86 | 18 | 11 | 21 | 124 | 3 | 259 |
| i-C ₄ H ₁₀ | 14 | 17 | 5 | 19 | 7 | 7 | 28 | 11 | 32 | 103 | 3 | 35 | 12 | 7 | 10 | 44 | 3 | 122 |
| n-C ₄ H ₁₀ | 18 | 19 | 6 | 24 | 8 | 7 | 28 | 6 | 41 | 144 | 3 | 53 | 14 | 8 | 15 | 66 | 3 | 163 |
| CH ₄ | 1800 | 1799 | 5 | 1809 | 1786 | 25 | 1762 | 1754 | 28 | 1836 | 1690 | 194 | 1757 | 1755 | 13 | 1799 | 1713 | 456 |
| C ₂ Cl ₄ | 5 | 5 | 0 | 5 | 4 | 7 | 4 | 2 | 3 | 15 | 1 | 88 | 2 | 2 | 1 | 6 | 1 | 279 |
| CCl ₄ | 99 | 100 | 1 | 100 | 98 | 7 | 99 | 99 | 1 | 103 | 97 | 88 | 98 | 98 | 1 | 101 | 95 | 279 |
| CH ₃ CCl ₃ | 39 | 40 | 1 | 40 | 38 | 7 | 40 | 39 | 2 | 45 | 37 | 88 | 39 | 39 | 1 | 41 | 38 | 279 |
| CH ₃ Cl | 620 | 624 | 23 | 654 | 588 | 7 | 582 | 567 | 41 | 709 | 536 | 88 | 569 | 561 | 32 | 641 | 525 | 279 |
| CH ₃ Br | 9 | 9 | 0 | 9 | 8 | 7 | 8 | 8 | 1 | 11 | 8 | 88 | 8 | 8 | 0 | 9 | 7 | 279 |
| CFC-11 | 260 | 260 | 1 | 261 | 259 | 7 | 260 | 260 | 2 | 268 | 256 | 88 | 258 | 258 | 2 | 263 | 254 | 279 |
| CFC-12 | 536 | 536 | 1 | 537 | 534 | 7 | 536 | 537 | 4 | 552 | 528 | 88 | 534 | 534 | 4 | 543 | 525 | 266 |
| CFC-113 | 79 | 79 | 1 | 80 | 78 | 7 | 79 | 79 | 1 | 82 | 77 | 88 | 79 | 79 | 1 | 81 | 77 | 279 |
| C ₂ H ₂ /CO | 2.26 | 2.24 | 0.23 | 2.51 | 1.82 | 7 | 1.50 | 1.01 | 0.98 | 4.13 | 0.63 | 83 | 1.15 | 1.01 | 0.47 | 2.74 | 0.63 | 250 |
| C ₃ H ₈ /C ₂ H ₆ | 0.10 | 0.10 | 0.01 | 0.12 | 0.09 | 7 | 0.08 | 0.06 | 0.05 | 0.24 | 0.03 | 88 | 0.08 | 0.06 | 0.04 | 0.20 | 0.02 | 279 |

^aMixing ratios are given in parts per trillion by volume except for O₃, CO, and CH₄ which are in parts per billion by volume and for CO₂ which is in parts per million by volume. The C₂H₂/CO ratio is in parts per trillion by volume/parts per billion by volume.

Table 4. Mixing Ratios of Selected Species From the NNW Source Region^a

| Species | <2 km | | | | | | 2–7 km | | | | | | >7 km | | | | | |
|--------------------------------------------------------------|-------|--------|-----------|------|------|-----|--------|--------|-----------|------|------|-----|-------|--------|-----------|------|------|----|
| | Mean | Median | Std. Dev. | Max | Min | N | Mean | Median | Std. Dev. | Max | Min | N | Mean | Median | Std. Dev. | Max | Min | N |
| O ₃ | 55 | 54 | 7 | 67 | 36 | 399 | 62 | 60 | 17 | 206 | 48 | 491 | 131 | 151 | 53 | 208 | 59 | 25 |
| CO | 204 | 207 | 25 | 266 | 136 | 368 | 145 | 126 | 46 | 420 | 74 | 443 | 103 | 105 | 9 | 118 | 88 | 25 |
| NO | 61 | 18 | 136 | 1450 | 0 | 297 | 33 | 10 | 78 | 465 | 0 | 402 | 56 | 55 | 28 | 97 | 22 | 17 |
| NO ₂ | 463 | 72 | 766 | 3349 | 0 | 190 | 51 | 27 | 63 | 664 | 1 | 402 | 23 | 23 | 13 | 40 | 5 | 17 |
| NO _y | 940 | 597 | 881 | 5115 | 12 | 391 | 397 | 260 | 397 | 3341 | 10 | 492 | 585 | 782 | 390 | 1230 | 88 | 24 |
| HNO ₃ | 447 | 436 | 195 | 1198 | 63 | 375 | 189 | 120 | 229 | 2028 | 49 | 452 | 456 | 543 | 349 | 1099 | 41 | 25 |
| PAN | 505 | 514 | 326 | 1422 | 1 | 160 | 293 | 193 | 229 | 998 | 89 | 229 | 116 | 124 | 28 | 151 | 80 | 16 |
| SO ₂ | 517 | 272 | 559 | 2821 | 4 | 328 | 403 | 42 | 1038 | 6989 | 7 | 398 | 31 | 24 | 17 | 70 | 12 | 18 |
| CO ₂ | 377 | 376 | 2 | 387 | 374 | 389 | 374 | 374 | 1.6 | 380 | 370 | 466 | 372 | 372 | 0.9 | 373 | 371 | 19 |
| H ₂ O ₂ | 543 | 425 | 442 | 2276 | 22 | 158 | 440 | 397 | 308 | 1058 | 30 | 210 | 96 | 90 | 59 | 201 | 22 | 10 |
| CH ₃ OOH | 169 | 111 | 172 | 1091 | 25 | 124 | 208 | 138 | 139 | 597 | 28 | 180 | 76 | 75 | 26 | 109 | 45 | 4 |
| CH ₂ O | 723 | 739 | 395 | 1935 | 83 | 113 | 292 | 138 | 400 | 1877 | 50 | 44 | 160 | 176 | 42 | 188 | 99 | 4 |
| C ₂ H ₆ | 2356 | 2353 | 407 | 3607 | 1276 | 135 | 1670 | 1646 | 411 | 2813 | 641 | 216 | 882 | 916 | 175 | 1076 | 597 | 14 |
| C ₂ H ₄ | 150 | 101 | 180 | 1228 | 19 | 134 | 38 | 15 | 59 | 318 | 3 | 179 | 5 | 5 | 2 | 8 | 3 | 8 |
| C ₂ H ₂ | 756 | 757 | 166 | 1205 | 268 | 135 | 398 | 304 | 211 | 1098 | 117 | 216 | 179 | 164 | 34 | 238 | 138 | 14 |
| C ₃ H ₈ | 859 | 804 | 310 | 1907 | 194 | 135 | 446 | 413 | 199 | 1115 | 96 | 216 | 149 | 133 | 60 | 232 | 71 | 14 |
| C ₆ H ₆ | 182 | 175 | 50 | 326 | 68 | 135 | 76 | 52 | 61 | 308 | 3 | 216 | 19 | 21 | 7 | 25 | 7 | 8 |
| i-C ₄ H ₁₀ | 144 | 130 | 71 | 386 | 20 | 135 | 60 | 52 | 35 | 189 | 8 | 216 | 7 | 6 | 3 | 12 | 4 | 14 |
| n-C ₄ H ₁₀ | 247 | 213 | 130 | 681 | 21 | 135 | 107 | 95 | 62 | 344 | 14 | 214 | 14 | 12 | 4 | 23 | 7 | 14 |
| CH ₄ | 1843 | 1841 | 17 | 1897 | 1803 | 318 | 1806 | 1802 | 22 | 1875 | 1750 | 438 | 1761 | 1760 | 11 | 1779 | 1744 | 25 |
| C ₂ Cl ₄ | 12 | 12 | 2 | 21 | 6 | 135 | 8 | 7 | 3 | 18 | 2 | 216 | 2 | 2 | 1 | 4 | 1 | 14 |
| CCl ₄ | 100 | 100 | 1 | 102 | 98 | 135 | 99 | 99 | 1 | 103 | 90 | 216 | 95 | 96 | 2 | 97 | 92 | 14 |
| CH ₃ CCl ₃ | 42 | 42 | 1 | 45 | 40 | 135 | 40 | 40 | 1 | 43 | 38 | 216 | 38 | 38 | 1 | 39 | 36 | 14 |
| CH ₃ Cl | 552 | 553 | 17 | 589 | 518 | 135 | 552 | 547 | 21 | 618 | 514 | 216 | 544 | 545 | 12 | 559 | 523 | 14 |
| CH ₃ Br | 9 | 9 | 1 | 18 | 9 | 135 | 9 | 9 | 1 | 11 | 8 | 216 | 9 | 9 | 0 | 9 | 8 | 14 |
| CFC-11 | 262 | 262 | 2 | 269 | 257 | 135 | 260 | 260 | 3 | 266 | 245 | 216 | 253 | 255 | 5 | 258 | 244 | 14 |
| CFC-12 | 540 | 540 | 3 | 549 | 530 | 135 | 537 | 538 | 4 | 550 | 518 | 216 | 530 | 532 | 8 | 537 | 517 | 14 |
| CFC-113 | 80 | 80 | 1 | 82 | 78 | 135 | 79 | 79 | 1 | 82 | 75 | 216 | 78 | 77 | 1 | 79 | 76 | 14 |
| C ₂ H ₂ /CO | 3.60 | 3.56 | 0.47 | 4.61 | 2.80 | 117 | 2.54 | 2.37 | 0.56 | 4.02 | 1.00 | 172 | 1.72 | 1.62 | 0.25 | 2.19 | 1.44 | 14 |
| C ₃ H ₈ /C ₂ H ₆ | 0.35 | 0.36 | 0.07 | 0.53 | 0.15 | 135 | 0.26 | 0.25 | 0.07 | 0.49 | 0.12 | 217 | 0.16 | 0.15 | 0.04 | 0.22 | 0.12 | 14 |

^aMixing ratios are given in parts per trillion by volume except for O₃, CO, and CH₄ which are in parts per billion by volume and for CO₂ which is in parts per million by volume. The C₂H₂/CO ratio is in parts per trillion by volume/parts per billion by volume.

Table 5. Mixing Ratios of Selected Species From the WSW Source Region^a

| Species | 2–7 km | | | | | | >7 km | | | | | |
|--------------------------------------------------------------|--------|--------|-----------|------|------|-----|-------|--------|-----------|------|------|-----|
| | Mean | Median | Std. Dev. | Max | Min | N | Mean | Median | Std. Dev. | Max | Min | N |
| O ₃ | 64 | 65 | 10 | 91 | 29 | 145 | 62 | 66 | 15 | 120 | 26 | 625 |
| CO | 110 | 108 | 17 | 175 | 78 | 136 | 134 | 121 | 48 | 281 | 70 | 556 |
| NO | 44 | 51 | 31 | 119 | 7 | 60 | 93 | 82 | 55 | 285 | 9 | 445 |
| NO ₂ | 45 | 43 | 19 | 83 | 10 | 52 | 29 | 24 | 21 | 149 | 2 | 358 |
| NO _y | 322 | 235 | 349 | 2257 | 5 | 140 | 297 | 245 | 211 | 1138 | 3 | 619 |
| HNO ₃ | 210 | 131 | 312 | 1987 | 33 | 128 | 121 | 100 | 83 | 762 | 25 | 518 |
| PAN | 187 | 187 | 63 | 341 | 78 | 67 | 268 | 181 | 186 | 699 | 44 | 246 |
| SO ₂ | 72 | 26 | 88 | 298 | 10 | 26 | 51 | 28 | 100 | 569 | 7 | 151 |
| CO ₂ | 372 | 372 | 1 | 373 | 371 | 131 | 372 | 372 | 2 | 376 | 369 | 521 |
| H ₂ O ₂ | 415 | 255 | 314 | 1091 | 94 | 60 | 205 | 193 | 125 | 589 | 22 | 215 |
| CH ₃ OOH | 170 | 195 | 70 | 286 | 25 | 47 | 120 | 98 | 91 | 540 | 25 | 141 |
| CH ₂ O | 262 | 189 | 272 | 1166 | 56 | 16 | 266 | 218 | 188 | 729 | 54 | 59 |
| C ₂ H ₆ | 824 | 893 | 191 | 1242 | 451 | 56 | 801 | 731 | 294 | 1569 | 295 | 260 |
| C ₂ H ₄ | 17 | 14 | 11 | 50 | 3 | 33 | 41 | 26 | 38 | 129 | 3 | 140 |
| C ₂ H ₂ | 211 | 190 | 108 | 602 | 81 | 56 | 291 | 208 | 219 | 930 | 47 | 260 |
| C ₃ H ₈ | 110 | 120 | 54 | 202 | 19 | 56 | 93 | 77 | 63 | 259 | 12 | 260 |
| C ₆ H ₆ | 31 | 24 | 23 | 107 | 7 | 56 | 46 | 30 | 43 | 179 | 3 | 223 |
| i-C ₄ H ₁₀ | 11 | 11 | 5 | 23 | 3 | 49 | 16 | 13 | 11 | 41 | 3 | 166 |
| n-C ₄ H ₁₀ | 19 | 20 | 9 | 36 | 3 | 51 | 21 | 14 | 18 | 65 | 3 | 203 |
| CH ₄ | 1767 | 1771 | 13 | 1794 | 1726 | 136 | 1771 | 1772 | 19 | 1831 | 1694 | 482 |
| C ₂ Cl ₄ | 3 | 3 | 1 | 6 | 2 | 56 | 3 | 2 | 2 | 12 | 0 | 260 |
| CCl ₄ | 98 | 98 | 1 | 101 | 96 | 56 | 98 | 98 | 2 | 101 | 87 | 260 |
| CH ₃ CCl ₃ | 39 | 39 | 1 | 41 | 37 | 56 | 39 | 39 | 2 | 41 | 31 | 260 |
| CH ₃ Cl | 568 | 566 | 19 | 621 | 538 | 56 | 595 | 588 | 29 | 668 | 543 | 260 |
| CH ₃ Br | 8 | 8 | 0 | 9 | 8 | 55 | 8 | 8 | 0.45 | 10 | 8 | 260 |
| CFC-11 | 259 | 259 | 2 | 263 | 255 | 56 | 258 | 257 | 2 | 264 | 253 | 260 |
| CFC-12 | 535 | 535 | 4 | 543 | 527 | 56 | 534 | 534 | 3 | 544 | 527 | 258 |
| CFC-113 | 79 | 79 | 1 | 87 | 77 | 56 | 79 | 79 | 1 | 81 | 73 | 260 |
| C ₂ H ₂ /CO | 1.88 | 1.82 | 0.63 | 4.49 | 0.98 | 52 | 1.95 | 1.59 | 0.80 | 3.81 | 0.67 | 229 |
| C ₃ H ₈ /C ₂ H ₆ | 0.13 | 0.13 | 0.04 | 0.21 | 0.04 | 56 | 0.10 | 0.10 | 0.04 | 0.21 | 0.03 | 260 |

^aMixing ratios are given in parts per trillion by volume except for O₃, CO, and CH₄ which are in parts per billion by volume and for CO₂ which is in parts per million by volume. The C₂H₂/CO ratio is in parts per trillion by volume/parts per billion by volume.

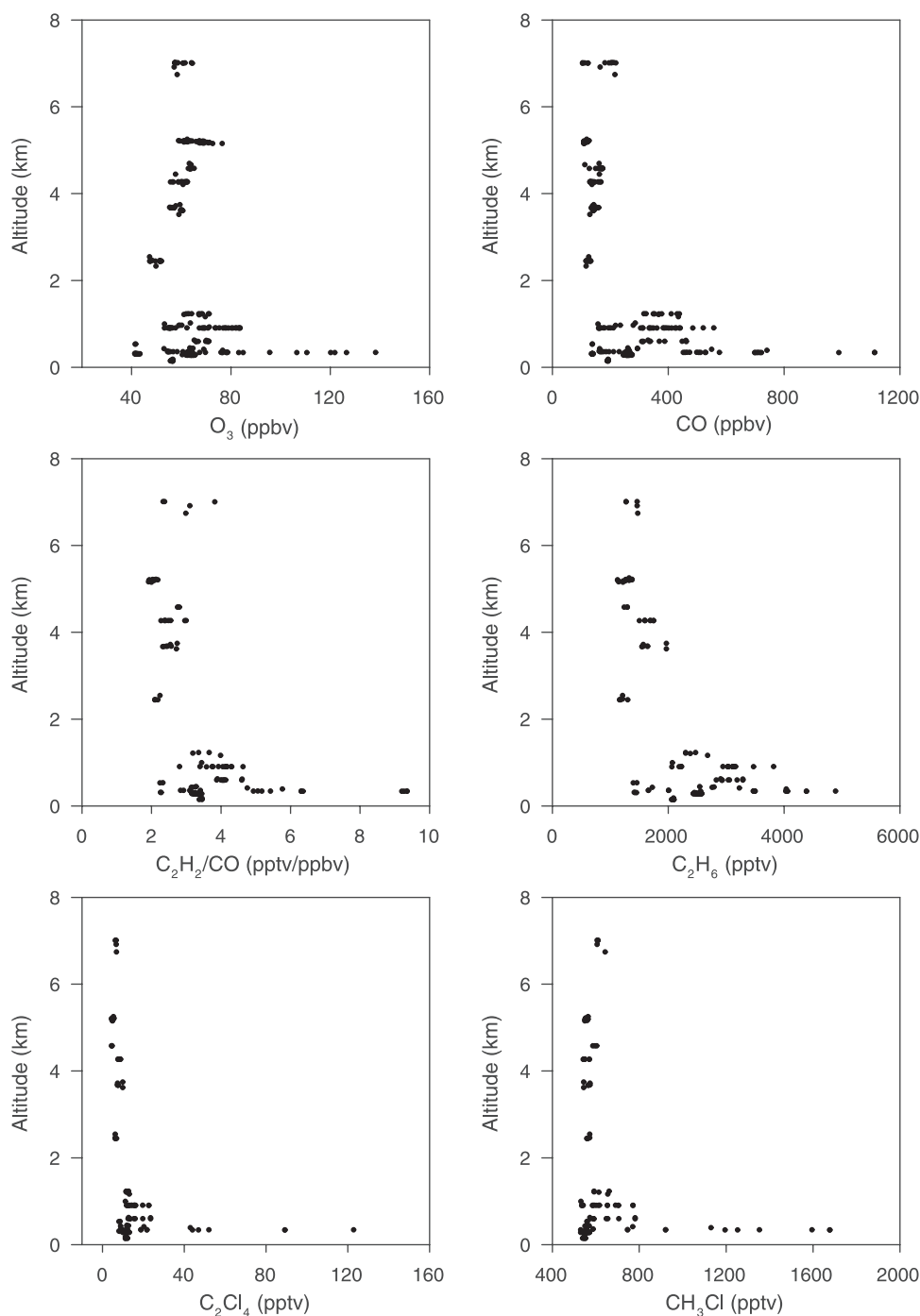


Figure 4. Vertical distributions of selected species in air masses originating in the Central source region.

plume [Na *et al.*, 2003]. These comparisons for polluted regions around the world suggest that the Shanghai plume is fairly representative of the magnitude of pollutants being transported from these large population centers.

[21] In the boundary layer outflow of the central region, CO was strongly correlated with C_2H_2 , C_2H_4 , and C_2H_6 ($r^2 \geq 0.86$). CO and C_2H_2 were also correlated with C_2Cl_4 ($r^2 = 0.77$ and 0.96 , respectively) and with CH_3Cl ($r^2 = 0.81$ and 0.90 , respectively). These results indicate that the outflow contained a complex mixture of fresh and processed emissions from combustion, industrial activities, and biomass/biofuel burning. This makes it difficult to distinguish

between fossil fuel and biofuel emissions. The strong correlations, particularly with C_2H_2 , were dominated by the emissions sampled directly from the Shanghai plume. Additional tracers have been identified which can specifically distinguish between Chinese (halon-1211) and Japanese/Korean (CH_3Br) emissions [Blake *et al.*, 2003]. Correlations between CO, C_2H_2 , and C_3H_8 with H-1211 ($r^2 = 0.72$ – 0.93) were stronger than the correlations with CH_3Br ($r^2 = 0.67$ – 0.76). As expected, these results suggest a stronger influence from Chinese sources in the boundary layer.

[22] Above the boundary layer, mixing ratios of most species were decreased significantly. The median CO and

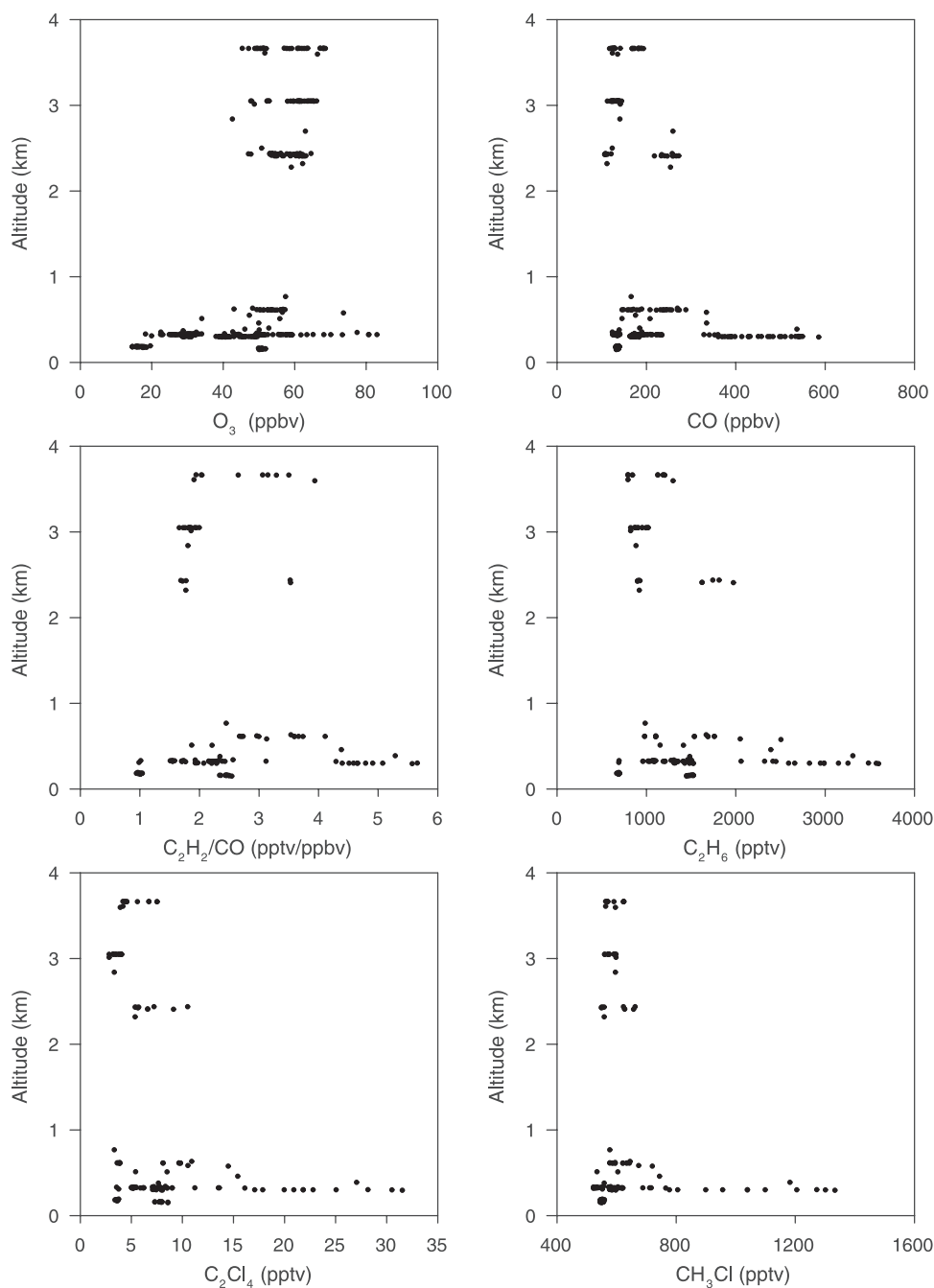


Figure 5. Vertical distributions of selected species in air masses originating in the Coastal source region.

NMHC mixing ratios were at least a factor of 2–3 lower in the middle altitudes compared to the boundary layer but they were still enhanced substantially above background levels. The hydrocarbon ratios were lower due to a lack of recent emission inputs and additional air mass processing and dilution. Correlations of CO and C₂H₂ with CH₃Cl ($r^2 = 0.83$ and 0.58 , respectively) indicate an influence from combustion and, in particular, biomass/biofuel burning emissions in the middle altitudes.

5.2. Coastal

[23] The middle altitudes of the coastal region only reflect data collected at 2–4 km while observations were available

for the other four regions from 2 to 7 km. Air masses in the coastal region had short transport distances to the western Pacific and apparently underwent minimal vertical uplifting. Aside from the differences in the air mass transport patterns and the strong dust influence in the central region [Jordan *et al.*, 2003], the chemistry of the central and coastal regions was essentially the same. The composition of the boundary layer in these two regions was directly influenced by recent emissions from anthropogenic activities in East Asia. Mixing ratios of CO, NMHCs, C₂Cl₄, and CH₃Cl were at least a factor of 3 higher than background (Figure 5, Table 2). Furthermore, O₃, PAN, NO_x, HNO₃, H₂O₂, and CH₃OOH were enhanced, suggestive of relatively recent photochem-

ical processing. This is supported by the strong correlation of CO and C₂H₂ with PAN ($r^2 \sim 0.85$). Recent (~ 1 day old) combustion inputs were present in the boundary layer outflow (C₂H₂/CO ~ 5 and C₃H₈/C₂H₆ ~ 0.5) along with extensively processed air. CO₂ and CH₄ were also enhanced in the boundary layer, and they were correlated with CO and C₂H₂ ($r^2 > 0.8$) suggesting an anthropogenic rather than biogenic source. In addition, CO₂ and CH₄ were correlated with combustion species ($r^2 > 0.6$) in the altitude ranges where outflow occurred in the other four source regions. *Vay et al.* [2003] analyzed eleven pollution plumes with CO₂ > 380 ppmv and CO > 250 ppbv and concluded that anthropogenic sources were responsible for the enhancements followed by frontal lifting associated with mid-latitude cyclones.

[24] In the middle altitudes, species mixing ratios decreased substantially, similar to those from the central region. Species, such as CO, C₂H₆, C₂H₄, C₂Cl₄, and CH₃Cl, were a factor of 2 or 3 lower compared to their maximum mixing ratios in the boundary layer. O₃, PAN, and H₂O₂ exhibited enhancements again showing significant photochemical processing. CO and C₂H₂ were well correlated with industrial tracer species, such as C₂Cl₄ ($r^2 > 0.91$ below 2 km and $r^2 \sim 0.7$ above 2 km). As found in the central region, CO and C₂H₂ were strongly correlated with CH₃Cl ($r^2 \geq 0.87$) in both altitude ranges. O₃ levels are often high in air masses containing aged biomass emissions [*Tang et al.*, 2003]. Biomass/biofuel burning may therefore explain the enhanced O₃ (~ 80 ppbv) observed in the boundary layer. Also, a combination of emissions from both Chinese and Japanese/Korean sources appear to be important as indicated by the strong correlations of CO, C₂H₂, C₂H₆, and C₃H₈ with both H-1211 and CH₃Br ($r^2 > 0.78$) in the boundary layer.

5.3. Southeast

[25] The SE region was characterized by two principal outflow regions, ~ 3 and 10 km (Figure 6). The outflow plume at 10 km altitude was especially impressive, with mixing ratios of CO exceeding 200 ppbv, C₂H₆ above 1000 pptv, and enhanced hydrocarbon ratios (C₂H₂/CO ~ 3 and C₃H₈/C₂H₆ ~ 0.2) (Table 3). Both outflow plumes had enhancements in CO, SO₂, NO_x, NMHCs, CH₃Cl, C₂Cl₄, CH₃CCl₃, and CCl₄. In the high-altitude outflow, water-soluble species, such as HNO₃, H₂O₂, and CH₃OOH, were not enhanced. In air masses that have recently been influenced by wet convection, the CH₃OOH/H₂O₂ ratio is usually >1 due to the greater solubility of H₂O₂ which is preferentially scavenged by precipitation [*Heikes*, 1992]. At high altitude, the CH₃OOH/H₂O₂ ratio was >1 , suggesting that wet convection lifted the emissions from the surface. This is consistent with the results from *Liu et al.* [2003] who suggested that the La Nina conditions during spring 2001 resulted in more frequent and stronger convection in SE Asia. This could be responsible for outflow of biomass burning emissions at high altitude. *Fuelberg et al.* [2003] also discuss the La Nina conditions during spring 2001 and its impact on transport patterns. O₃ had a wide range of mixing ratios varying from 20 to 70 ppbv at all altitudes. The enhanced O₃ mixing ratios at high altitude may be attributed to photochemical production from the uplifted biomass burning emissions. Extensively processed air

masses containing background air with low hydrocarbon ratios were also encountered above 2 km.

[26] The highest mixing ratios of H₂O₂ and CH₃OOH originated from the SE source region at altitudes of up to ~ 3 km. The median mixing ratios of H₂O₂ and CH₃OOH in the boundary layer were a factor of 4–15 larger than the medians in the other three source regions that had boundary layer data (i.e., central, coastal, NNW). Areas affected by significant biomass burning outflow, such as over the South Atlantic, have been found to contain considerably enhanced mixing ratios of H₂O₂ and CH₃OOH due to efficient photochemical production [*Talbot et al.*, 1996b; *Heikes et al.*, 1996]. Mixing ratios of NO₂, PAN, and HNO₃ were enhanced in the 3 km outflow, but NO was not enhanced presumably due to conversion to other reactive nitrogen species. This indicates that combustion was a significant source of reactive nitrogen in the Asian outflow.

[27] An anthropogenic influence was apparent in all three altitude ranges, with the strongest correlations found in the middle altitudes where CO was highly correlated with C₂H₂, C₂H₆, C₂Cl₄, and CH₃Cl ($r^2 \geq 0.89$). CH₃Cl has also been found to have an oceanic source [*Khalil et al.*, 1999] which may have made a minor contribution to the enhancements observed in the SE, central, and coastal regions. However, the correlations with the combustion species in these regions argue strongly for an anthropogenic source of CH₃Cl. Furthermore, biomass burning has been found to be a larger source of CH₃Cl than the ocean [*Lobert et al.*, 1999; *Khalil et al.*, 1999]. HCN has also been proposed to be a good tracer of biomass burning [*Singh et al.*, 2003; *Li et al.*, 2003]. Correlations of CH₃Cl, CO, C₂H₆, and C₂H₂ with HCN ($r^2 \geq 0.7$) are relatively strong providing further evidence of a significant impact from biomass burning in the SE region. Furthermore, it is likely that biomass burning made a large contribution because spring is the dry season in Asia and extensive biomass burning occurs at this time of year in India and SE Asia [e.g., *Bey et al.*, 2001; *Blake et al.*, 1997]. Several companion papers have also found evidence of substantial biomass burning emissions being transported from SE Asia. For instance, *Heald et al.* [2003] concluded that biomass burning was responsible for approximately 30% of the CO emissions south of 30°N. *Carmichael et al.* [2003a] also found that biomass burning emissions were transported from SE Asia above 2 km and below 30°N.

5.4. North-Northwest

[28] The vertical distributions for the NNW region show that outflow occurred at several altitudes between 2 and 8 km with several species exhibiting a general decreasing trend with altitude (Figure 7). Mixing ratios of CO, C₂Cl₄, and NMHCs decreased by factors of 3–4 from the boundary layer to the upper troposphere (Table 4). NO was enhanced (465 pptv) at ~ 7.5 km with coincident enhancements in several species, such as CO, C₂H₆, C₂H₂, CH₃Cl, and C₂Cl₄, suggesting that recent surface emissions were lifted to this altitude. The composition of the upper troposphere of the NNW region was influenced by a mixture of stratospheric and surface level air. O₃ and CO were both enhanced with mixing ratios of ~ 100 ppbv and higher. Also, the air masses were freshest at low altitude,

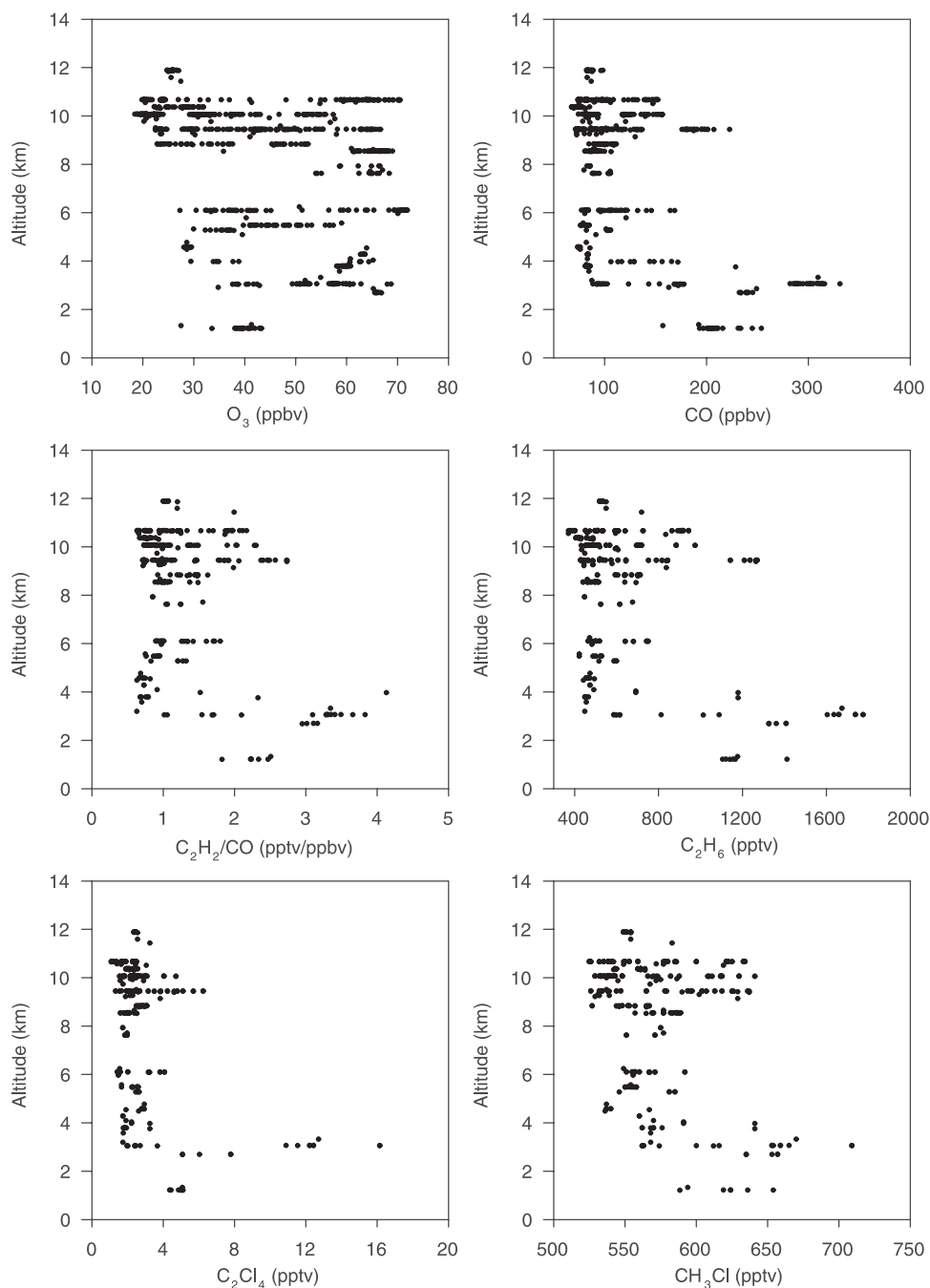


Figure 6. Vertical distributions of selected species in air masses originating in the Southeast source region.

and the relative age generally increased with altitude reflecting both stratospheric and aged surface emissions at the highest altitudes.

[29] Aged and diluted industrial and biomass/biofuel burning emissions were mixed with recent combustion emissions in the boundary layer. CO was weakly correlated with C₂Cl₄ and CH₃Cl ($r^2 < 0.3$) below 2 km, however, correlations of CO and C₂H₆ with C₂H₂ ranged from $r^2 = 0.74$ to 0.92 at low and middle altitudes. Emissions from industrial activity impacted the middle altitudes where CO and C₂H₂ were fairly well correlated with C₂Cl₄ ($r^2 = 0.68$ and 0.84 , respectively).

[30] The presence of middle and high altitude outflow in the NNW, SE, and WSW regions undoubtedly reflects the longer transport distance for air masses which allows uplift and entrainment of continental emissions. Furthermore, these air masses may contain more processed and diluted emissions because of the long distance from source inputs. The relatively strong anthropogenic influence in and above the boundary layer of the NNW region may be from the uplift of emissions from the central region as the air masses passed over it on route to the western Pacific. Since the DC-8 did not sample over the Asian continent, there is really no way to separate these potential confounding influences

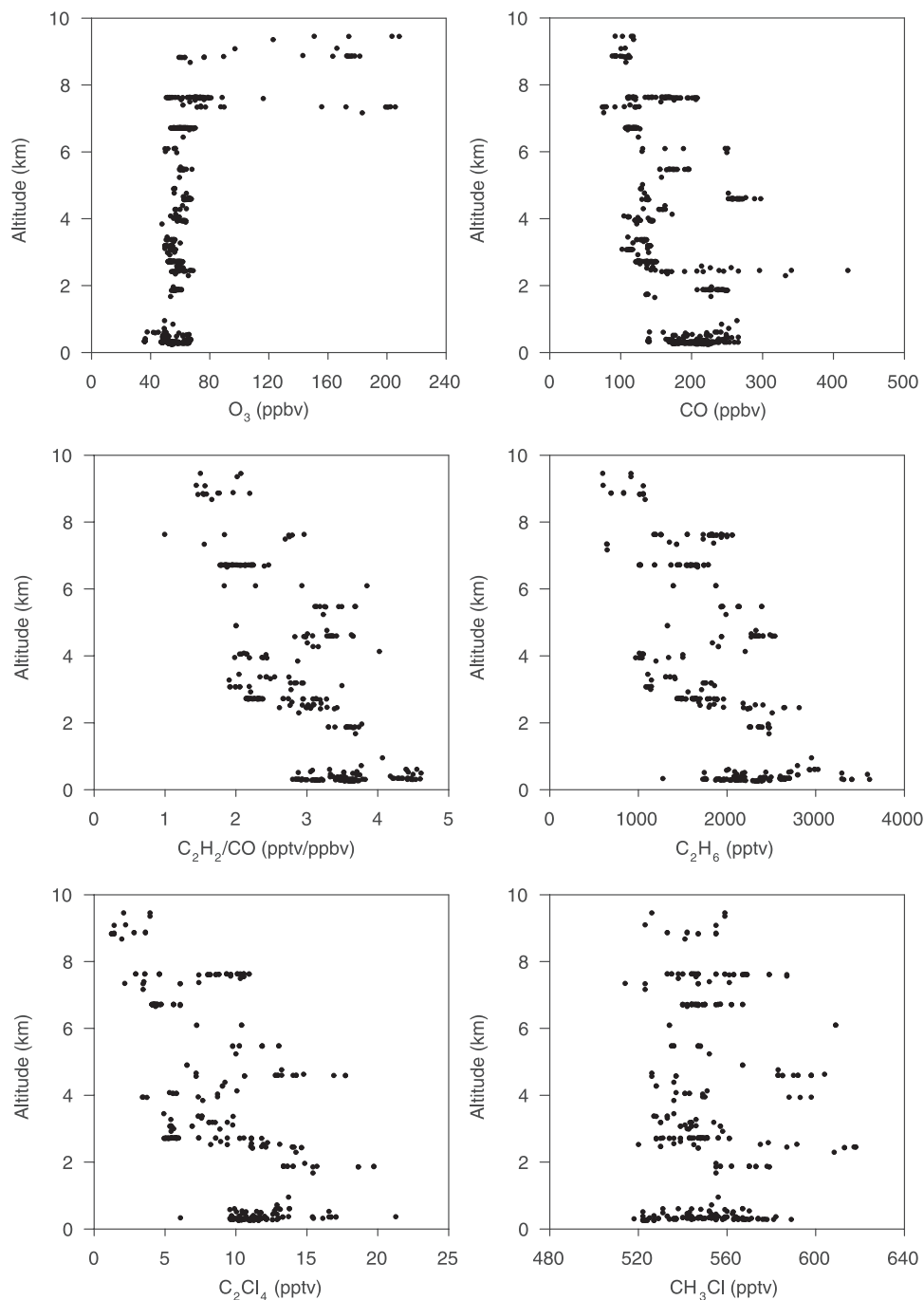


Figure 7. Vertical distributions of selected species in air masses originating in the North-Northwest source region.

from the two source regions. However, these two regions are kept separate because the NNW region trajectories originated at a much greater distance from the western Pacific. In addition, *Jordan et al.* [2003] demonstrated that the aerosol composition of the central region contained significantly more Ca^{+2} which separates it uniquely from the NNW region. Another possible explanation is transport of pollution from Europe or western Asia. However, only a small amount of the back trajectories in the NNW region originated over Europe [*Fuelberg et al.*, 2003]. This suggests that the long-range transport of European emissions was not significant

but nevertheless may have contributed to the air mass composition. Surface data has found evidence of a large CO plume from European fossil fuel combustion that is advected eastward over Siberia in the spring [*Rockmann et al.*, 1999]. Also, surface level data from the NOAA/CMDL sites in eastern Europe have found maximum CO mixing ratios to occur in the late winter/spring [e.g., *Novelli et al.*, 1998]. Previous work in the western Pacific has found evidence of a European pollution signal in Asian continental outflow. For example, the transport of European emissions to the western Pacific was a possible cause of high-altitude

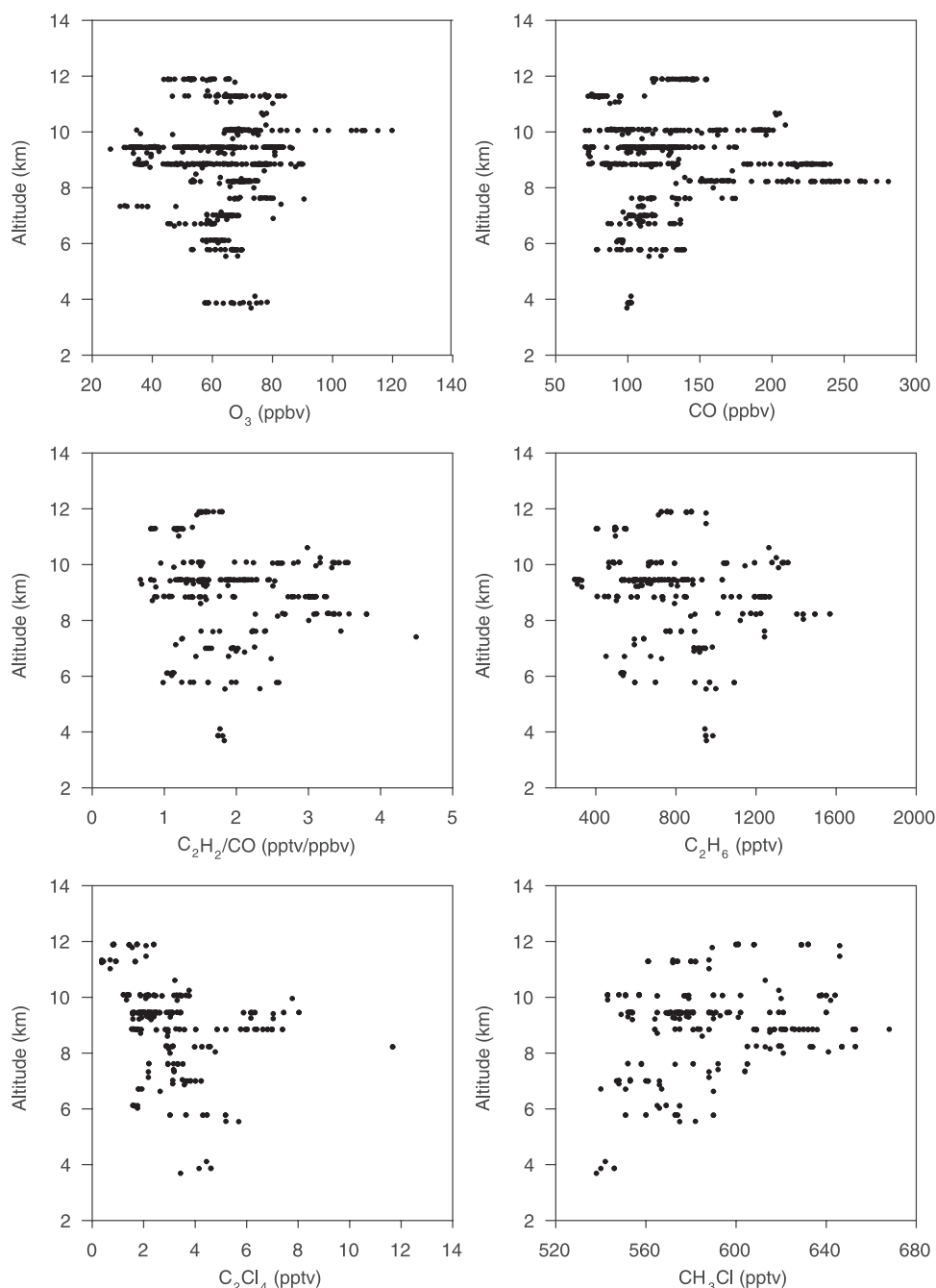


Figure 8. Vertical distributions of selected species in air masses originating in the West-Southwest source region.

species enhancements in the continental north group during PEM-West B [Talbot *et al.*, 1997]. In addition, anthropogenic emissions from Europe have been found to contribute significantly to Asian outflow at latitudes north of 40°N [Bey *et al.*, 2001]. However, any European influence south of 40°N indicated by 3-D simulations of CO mixing ratios was undetectable due to the strong Asian pollution signal [Liu *et al.*, 2003].

5.5. West-Southwest

[31] The WSW region only exhibited continental outflow in the middle and upper altitudes. The vertical distributions

in the WSW and SE regions were similar in that significant outflow was present at high altitude (Figure 8, Table 5). Outflow from the WSW region occurred between 8 and 10 km. The $\text{CH}_3\text{OOH}/\text{H}_2\text{O}_2$ ratio was occasionally >1 in the outflow suggesting that some of the surface emissions may have been lifted by wet convection. Also, the lifting of emissions by midlatitude cyclones and their associated fronts appears to have been important for exporting emissions from the WSW region. This was the dominant transport pathway during TRACE-P [Liu *et al.*, 2003]. Furthermore, the $\text{C}_2\text{H}_2/\text{CO}$ (>3) and $\text{C}_3\text{H}_8/\text{C}_2\text{H}_6$ (~ 0.2) ratios were enhanced above 7 km indicating that the outflow

contained relatively recent combustion inputs. As found in the SE region, background mixing ratios of several species, such as CO, O₃, C₂H₆, C₂H₂, C₃H₈, C₂Cl₄, and CH₃Cl, were also present intermittently in both the middle and upper troposphere indicating that substantial atmospheric processing had occurred. The similarities between the air mass composition in the WSW and SE regions may be a result of convective uplift of emissions from the SE region where they became entrained in the WSW region outflow.

[32] A striking feature of the WSW region is that both NO and CH₃Cl mixing ratios increased with altitude. The highest mixing ratios of NO were observed between 11 and 12 km, possibly from stratospheric inputs, lightning, or aircraft exhaust. Mixing ratios of O₃ (120 ppbv) and CO (~200 ppbv) were also enhanced around 10 km implying that these high-altitude air parcels contained a mixture of stratospheric and polluted air. *Talbot et al.* [2003] found that relationships between NO_x, O₃, and HNO₃ suggest a stratospheric source was responsible for enhanced NO_x in the upper troposphere. These results are consistent with data collected during the CARIBIC aircraft campaign that studied air masses at 10–11 km between Germany and the Indian Ocean [*Zahn et al.*, 2002]. This study area includes a portion of the WSW region. The CARIBIC study found that stratospheric inputs and photochemical production contributed equally to O₃ levels in the spring at middle latitudes. In contrast, photochemical production was responsible for the majority of the high-altitude O₃, with stratospheric inputs having a minimal influence, in the tropics [*Zahn et al.*, 2002]. This supports that both stratospheric and continental air was present in the upper troposphere of the WSW region and provides evidence that there are differences in the chemistry of the WSW and SE regions.

[33] NO and CH₃Cl were poorly correlated ($r^2 < 0.1$) above 7 km suggesting that biomass burning emissions were not responsible for the enhanced NO. *Liu et al.* [2003] concluded that CO emissions from African biomass burning were not detectable in air masses from the WSW region because any signal would be masked by the significant Asian pollution sources. Vertical lifting of emissions from the SE region is the most likely explanation for the enhanced CH₃Cl in the upper troposphere. However, an African contribution cannot be completely ruled out because a significant amount of the 5-day back trajectories in the WSW region originated over Africa. Also, biomass burning emissions from Africa have been shown to make a major contribution to Asian outflow at low latitudes and in the middle and upper troposphere [*Bey et al.*, 2001], and sources in the Middle East may have contributed to high-altitude outflow during PEM-West B [*Talbot et al.*, 1997].

[34] Recently injected anthropogenic emissions had a minimal influence on the composition of the middle troposphere in the WSW region. These air masses were aged several days and lacked strong correlations between key tracer species. C₂Cl₄ mixing ratios were enhanced ~9 km (~12 pptv), however, it was poorly correlated with CO and C₂H₂ ($r^2 < 0.4$ at middle and high altitudes) which is indicative of aged industrial emissions. Similar to the SE region, the high altitude outflow contained combustion and biomass/biofuel burning emissions as indicated by correlations of CO, C₂H₂, and C₂H₆ with CH₃Cl ($r^2 \sim 0.62$ – 0.71). Furthermore, C₂H₂ and C₂H₆ were moderately correlated

with the biomass burning tracer, HCN ($r^2 = 0.78$ and 0.74 , respectively). Among the high altitudes of the WSW, NNW, and SE regions, the highest mean and median mixing ratios of CO, C₂H₄, C₂H₂, C₆H₆, CH₃Cl, SO₂, PAN, and H₂O₂ were in air masses from the WSW region. Except for SO₂, these species are all characteristic of biomass burning. According to *Streets et al.* [2003], India is the second largest Asian source of SO₂, with power generation and industry being the largest sectors, and thus is a possible source of the enhanced SO₂. Similar results were found by the INDOEX campaign in 1999. Examination of air masses from India and SE Asia also found a minor contribution from industrial sources (low C₂Cl₄ and CH₃CCl₃) and an important influence in the free troposphere from biomass burning sources [*Scheeren et al.*, 2002].

6. Comparison With PEM-West B

[35] The TRACE-P and PEM-West B missions both occurred in late winter and spring but were conducted seven years apart. *Fuelberg et al.* [2003] concluded that the meteorological scenarios during the two missions were fairly similar; therefore meteorology most likely had a minimal influence on any variations in the tropospheric chemistry. Differences in the timing and design of the missions must also be considered. TRACE-P began later in February and lasted for a longer period of time than PEM-West B. As a result, the chemical composition may be influenced more by the characteristics of the springtime troposphere [*Fuelberg et al.*, 2003]. Furthermore, *Dibb et al.* [2003] suggest that the direct sampling of continental outflow, specifically near the Yellow Sea and the coast of China, during TRACE-P is a significant factor explaining different chemical and aerosol distributions between the two missions. This area was not probed during PEM-West B, and it clearly is a region heavily polluted by continental outflow.

[36] The three altitude ranges used in this paper are the same ranges used to characterize outflow during PEM-West B, thus allowing the vertical distributions to be compared. *Talbot et al.* [1997] separated the data at 20°N latitude into continental north and continental south groups. The NNW, central, coastal, and WSW regions are located at more northern latitudes and can thus be compared with the continental north group, and the SE and continental south regions can also be compared more or less directly. The median, maximum, and minimum mixing ratios of selected species are compared for the two missions in Tables 6–8. The “All” column represents all data from Flights 6–17 of TRACE-P, including data collected during spiral maneuvers. The WSW region is not included in the <2 km table (Table 6) because no boundary layer outflow was sampled. The central and coastal regions are not included in the >7 km table (Table 8) because they did not have high-altitude outflow due to their proximity to the flight paths.

6.1. Northern Regions

[37] The most striking difference between the two missions is that in all three altitude ranges the median O₃ mixing ratios were generally ~10–20 ppbv higher during TRACE-P. Although the seasonal timing of the two missions was fairly similar, TRACE-P did extend two weeks

Table 6. Comparison of Mixing Ratios for Selected Species From the TRACE-P and PEM-West B Missions for Data <2 km^a

| | | All | Central | Coastal | NNW | PEM West B-North | SE | PEM West B-South |
|--------------------------------|--------|-------|---------|---------|------|---------------------|------|---------------------|
| O ₃ | Median | 53 | 64 | 43 | 54 | 42 | 40 | 41 |
| | Max | 138 | 138 | 83 | 67 | 144 | 43 | 76 |
| | Min | 15 | 41 | 15 | 36 | 34 | 27 | 16 |
| CO | Median | 201 | 264 | 166 | 207 | 186 | 205 | 187 |
| | Max | 1113 | 1113 | 586 | 266 | 623 | 254 | 260 |
| | Min | 99 | 135 | 124 | 136 | 145 | 157 | 125 |
| C ₂ H ₂ | Median | 643 | 860 | 384 | 757 | 792 | 456 | 464 |
| | Max | 10403 | 10403 | 3264 | 1205 | 3356 | 627 | 835 |
| | Min | 122 | 308 | 125 | 268 | 463 | 369 | 176 |
| C ₂ H ₆ | Median | 2079 | 2540 | 1353 | 2353 | 2294 | 1155 | 1053 |
| | Max | 4888 | 4888 | 3598 | 3607 | 4323 | 1412 | 1528 |
| | Min | 661 | 1396 | 669 | 1276 | 1582 | 1105 | 655 |
| SO ₂ | Median | 348 | 2621 | 48 | 272 | 104 | 20 | 68 |
| | Max | 30736 | 30736 | 1554 | 2821 | 29770 | 45 | 2290 |
| | Min | 4 | 353 | 4 | 4 | 26 | 7 | 52 |
| C ₂ Cl ₄ | Median | 11 | 12 | 8 | 12 | 20 | 5 | 7.6 |
| | Max | 123 | 123 | 32 | 21 | 50 | 5 | 13 |
| | Min | 3 | 8 | 3 | 6 | 9 | 4 | 5.4 |

^aThe All column refers to all data from Flights 6–17. Units are in pptv except for O₃ and CO which are in ppbv.

more into the springtime than PEM-West B which may result in increased O₃ production. Several companion papers found that this seasonal difference could be an important factor explaining the observed trace gas distributions during TRACE-P compared with PEM-West B [e.g., Blake *et al.*, 2003; D. D. Davis *et al.*, Trends western North-Pacific ozone photochemistry as defined by observations from NASA's PEM-West B [1994] and TRACE-P [2001] field studies, submitted to *Journal of Geophysical Research*, 2003].

[38] Another noticeable difference between the two missions was the approximate factor of 2 lower mixing ratios of C₂Cl₄ during TRACE-P. This is likely a reflection of reduced emissions of industrial species, such as C₂Cl₄, CH₃CCl₃, and CCl₄, in Asia [Blake *et al.*, 2003]. CO mixing ratios were somewhat higher during TRACE-P at both low and high altitude. In the middle troposphere, CO mixing ratios were fairly similar particularly when comparing the heavily polluted central and coastal regions with the continental north group. At low and middle altitudes, C₂H₂ and C₂H₆ were generally lower during TRACE-P than they were during PEM-West B possibly because of increased OH oxidation in the spring or better emission controls in East Asia [Streets *et al.*, 2003]. The only exception is the central group in which C₂H₂ and C₂H₆ had higher median and maximum mixing ratios in the boundary layer due to the Shanghai plume. The median SO₂ mixing ratios were significantly larger in the low and middle altitudes of the “All,” central, and NNW groups during TRACE-P. This result is unexpected given that Streets *et al.* [2003] estimated a 17.2% reduction in SO₂ emissions during 1994–2001 in East Asia. The fact that the higher median SO₂ mixing ratios were in the central and NNW regions may be evidence of the importance of the extensive sampling over the Yellow Sea during TRACE-P as explained by Dibb *et al.* [2003]. Also, China still dominates Asian sulfur emissions [Streets *et al.*, 2003] which may be a factor. Furthermore, ground based data

Table 7. Comparison of Mixing Ratios for Selected Species From the TRACE-P and PEM-West B Missions for Data Between 2 and 7 km^a

| | | All | Central | Coastal | NNW | WSW | PEM West B-North | SE | PEM West B-South |
|--------------------------------|--------|------|---------|---------|------|------|---------------------|------|---------------------|
| O ₃ | Median | 59 | 61 | 60 | 60 | 65 | 45 | 57 | 56 |
| | Max | 206 | 76 | 69 | 206 | 91 | 69 | 72 | 66 |
| | Min | 19 | 47 | 43 | 48 | 29 | 23 | 27 | 16 |
| CO | Median | 122 | 135 | 132 | 126 | 108 | 138 | 88 | 88 |
| | Max | 530 | 219 | 272 | 420 | 175 | 300 | 331 | 203 |
| | Min | 70 | 104 | 107 | 74 | 78 | 72 | 74 | 81 |
| C ₂ H ₂ | Median | 252 | 313 | 255 | 304 | 190 | 471 | 93 | 65 |
| | Max | 2233 | 645 | 908 | 1098 | 602 | 1481 | 1210 | 847 |
| | Min | 46 | 209 | 181 | 117 | 81 | 28 | 48 | 50 |
| C ₂ H ₆ | Median | 1078 | 1334 | 929 | 1646 | 893 | 1614 | 528 | 555 |
| | Max | 3441 | 1968 | 1974 | 2813 | 1242 | 3771 | 1775 | 1601 |
| | Min | 401 | 1125 | 793 | 641 | 451 | 469 | 422 | 468 |
| SO ₂ | Median | 38 | 65 | 21 | 42 | 26 | 22 | 23 | 12 |
| | Max | 6989 | 284 | 120 | 6989 | 298 | 1432 | 415 | 26 |
| | Min | 5 | 10 | 10 | 7 | 10 | 5 | 6 | 12 |
| C ₂ Cl ₄ | Median | 4 | 6 | 5 | 7 | 3 | 13 | 2 | 5 |
| | Max | 115 | 10 | 11 | 18 | 6 | 27 | 16 | 8 |
| | Min | 1 | 4 | 3 | 2 | 2 | 3.4 | 1 | 4 |

^aThe All column refers to all data from Flights 6–17. Units are in pptv except for O₃ and CO which are in ppbv.

from the south China coast found similar results with higher O₃ and SO₂ during TRACE-P [Wang *et al.*, 2003].

6.2. Southern Regions

[39] A similarity between both missions is that mixing ratios for the six species used in this comparison were generally lower in the SE and continental south groups than in the northern TRACE-P regions and the continental north group. This is likely a result of the industrial cities and strong westerly outflow north of 20°N. In contrast to the northern groups, the median O₃ mixing ratios in the SE and continental south groups were remarkably similar in all altitude ranges. CO demonstrated the same trend as in the northern groups, with larger mixing ratios at low and high altitude during TRACE-P and with similar mixing ratios at middle altitudes.

Table 8. Comparison of Mixing Ratios for Selected Species From the TRACE-P and PEM-West B Missions for Data >7 km^a

| | | All | NNW | WSW | PEM West B-North | SE | PEM West B-South |
|--------------------------------|--------|------|------|------|---------------------|------|---------------------|
| O ₃ | Median | 53 | 151 | 66 | 51 | 32 | 35 |
| | Max | 208 | 208 | 120 | 119 | 70 | 69 |
| | Min | 18 | 59 | 26 | 25 | 18 | 21 |
| CO | Median | 102 | 105 | 121 | 94 | 88 | 81 |
| | Max | 341 | 118 | 281 | 316 | 223 | 111 |
| | Min | 63 | 88 | 70 | 62 | 67 | 57 |
| C ₂ H ₂ | Median | 146 | 164 | 208 | 131 | 89 | 67 |
| | Max | 1132 | 238 | 930 | 1513 | 609 | 274 |
| | Min | 47 | 138 | 47 | 35 | 47 | 16 |
| C ₂ H ₆ | Median | 631 | 916 | 731 | 672 | 514 | 543 |
| | Max | 1911 | 1076 | 1569 | 2463 | 1270 | 912 |
| | Min | 295 | 597 | 295 | 439 | 370 | 280 |
| SO ₂ | Median | 24 | 24 | 28 | 22 | 21 | 23 |
| | Max | 569 | 70 | 569 | 62 | 284 | 57 |
| | Min | 7 | 12 | 7 | 5 | 10 | 5 |
| C ₂ Cl ₄ | Median | 2 | 2 | 2 | 22 | 2 | 4.1 |
| | Max | 12 | 4 | 12 | 62 | 6 | 7.9 |
| | Min | 0 | 1 | 0 | 5 | 1 | 1.4 |

^aThe All column refers to all data from Flights 6–17. Units are in pptv except for O₃ and CO which are in ppbv.

Table 9. Comparison of Species Ratios for the Five TRACE-P Source Regions and the 2000 Asian Emissions Summary

| Location | CO/CO ₂ | CO/CH ₄ | NO _x /SO ₂ | C ₂ H ₆ /C ₃ H ₈ |
|--------------------------|-------------------------------------|-------------------------------------|-------------------------------------------------------------------|--------------------------------------------------------------|
| <i>Emissions Summary</i> | | | | |
| China | 0.048 | 1.8 | 0.8 | 2.1 |
| Other East Asia | 0.014 | 2.2 | 2.7 | 1.3 |
| Japan | 0.009 | 3.7 | 3.8 | 1.1 |
| Rep. of Korea | 0.011 | 1.1 | 2.2 | 1.1 |
| SE Asia | 0.061 | 1.9 | 1.7 | 3.8 |
| South Asia | 0.054 | 1.1 | 1.1 | 2.7 |
| India | 0.053 | 1.1 | 1.2 | 2.6 |
| <i>TRACE-P</i> | | | | |
| | $\Delta\text{CO}/\Delta\text{CO}_2$ | $\Delta\text{CO}/\Delta\text{CH}_4$ | $\frac{\Delta\text{NO}_y}{\Delta(\text{SO}_2 + \text{nss SO}_4)}$ | $\Delta\text{C}_2\text{H}_6/\Delta\text{C}_3\text{H}_8$ |
| Central | 0.022 | 1.6 | 0.3 | 2.6 |
| Coastal | 0.017 | 1.4 | 0.7 | 4.2 |
| SE | 0.013 | 3.4 | 4.8 | 5.2 |
| NNW | 1.017 | 1.4 | 0.5 | 2.8 |
| WSW | 0.020 | 2.1 | 3.6 | 5.2 |

In the middle troposphere, both the SE and continental south groups had a median CO value of 88 ppbv. C₂H₂, C₂H₆, and SO₂ did not exhibit any definite trends between the two missions. At low altitudes, C₂H₂ was fairly similar during the two missions while it appears higher in the SE group at middle and high altitudes. At low altitudes, SO₂ was significantly lower in the SE region compared to the continental south group. At high altitude in the WSW and SE regions, instances of significantly enhanced SO₂ were encountered as indicated by high maximum mixing ratios, but this did not occur in the upper troposphere during PEM-West B. C₂Cl₄ was also lower in the SE region than in the PEM-West B continental south group presumably reflecting reduced emissions of industrial species.

7. Comparison of Source Regions With Emissions Summary

[40] In order to gain insight on how well the 2000 Asian anthropogenic emissions summary developed by *Streets et al.* [2003] represented the Asian continent and how representatively the DC-8 sampled Asian outflow, emission ratios were compared with species ratios from each of the five source regions identified and characterized in this paper. The $\Delta\text{CO}/\Delta\text{CO}_2$, $\Delta\text{CO}/\Delta\text{CH}_4$, $\Delta\text{C}_2\text{H}_6/\Delta\text{C}_3\text{H}_8$, and $\Delta\text{NO}_y/\Delta(\text{SO}_2 + \text{nss-SO}_4)$ ratios for each of the five source regions were compared with the ratios from the emissions summary. The Δ refers to the difference between the measured and background mixing ratios and represents the impact from Asian emissions. The emissions summary provides data for NO_x and SO₂, so the NO_x/SO₂ ratio was compared with the observed $\Delta\text{NO}_y/\Delta(\text{SO}_2 + \text{nss-SO}_4)$ ratio. This latter ratio accounts for conversion of primary nitrogen and sulfur species present in the atmosphere after emission from various sources. Here nss-SO₄ represents non-sea-salt sulfate as presented by *Dibb et al.* [2003].

[41] The total anthropogenic emissions data was used from the emissions inventory. The median mixing ratios of all the data for each species in the five TRACE-P source regions were used in the calculations. Background mixing ratios were determined from Flight 5 as discussed previously in this paper. The background mixing ratios used were: CO = 70 ppbv, CO₂ = 370 ppmv, CH₄ = 1750 ppbv,

C₂H₆ = 420 pptv, C₃H₈ = 15 pptv, SO₂ + nss-SO₄ = 50 pptv, and NO_y = 60 pptv. These ratios only provide a rough comparison of the emissions summary and the TRACE-P data. The TRACE-P measurements were collected from several altitudes while the emission summary ratios may be more representative of surface measurements. TRACE-P ratios using only <2 km data were calculated and compared with the ratios using all the data from the three altitude ranges. There was very little difference between the ratios so we used the larger data set composed of the data from all three altitude bins. Also, the five source regions identified in this paper and the regions used in the emissions inventory are not exactly the same. Furthermore, the emission summary represents an entire year, but the TRACE-P source regions are only representative of 6 weeks of data. However, *Streets et al.* [2003] concluded that emissions during the TRACE-P period were near their average values.

[42] In general, there was remarkably good agreement and correspondence between the ratios for our five source regions and the emissions summary (Table 9). All calculated TRACE-P ratios were generally within the same order of magnitude as the emission summary ratios. The $\Delta\text{CO}/\Delta\text{CO}_2$ ratio for TRACE-P was ~ 0.02 in all five source regions which is within the estimated range of emission ratios, ~ 0.01 – 0.06 . Both the CO/CH₄ and $\Delta\text{CO}/\Delta\text{CH}_4$ ratios were between 1 and 4, and both the C₂H₆/C₃H₈ and $\Delta\text{C}_2\text{H}_6/\Delta\text{C}_3\text{H}_8$ ratios were between ~ 1 and 5.2 for all regions compared. *Carmichael et al.* [2003b] examined numerous chemical species ratios using both observed and modeled results and found that high values of the C₂H₆/C₃H₈ ratio (~ 8) are representative of biomass burning in SE Asia while a lower ratio value (~ 2) reflects biofuel combustion. The $\Delta\text{C}_2\text{H}_6/\Delta\text{C}_3\text{H}_8$ values are highest in the SE and WSW source regions (~ 5.2), and the highest C₂H₆/C₃H₈ values from the emissions inventory are in the SE and South Asia groups, which is somewhat consistent with the *Carmichael et al.* [2003b] results. The $\Delta\text{C}_2\text{H}_6/\Delta\text{C}_3\text{H}_8$ ratio value in the central and NNW regions is ~ 2.7 which is near the expected value due to the higher use of fossil fuels and biofuels in central China.

[43] The $\Delta\text{CO}/\Delta\text{CO}_2$, $\Delta\text{CO}/\Delta\text{CH}_4$, $\Delta\text{C}_2\text{H}_6/\Delta\text{C}_3\text{H}_8$, and $\Delta\text{NO}_y/\Delta(\text{SO}_2 + \text{nss-SO}_4)$ ratios in the central and coastal regions were similar and comparable to the respective ratios

from the China region. For example, the NO_x/SO_2 ratio value of 0.77 for China is very comparable with the $\Delta\text{NO}_y/\Delta(\text{SO}_2 + \text{nss-SO}_4)$ ratios of 0.30 and 0.73 for the central and coastal regions, respectively. These ratio values are consistent with the observed NO_y/SO_x values ($\sim 0.2\text{--}0.5$) for Chinese cities from Carmichael *et al.* [2003b]. The values are also fairly similar with the NO_x/SO_2 ratio (~ 0.31) based on emission estimates of Kato and Akimoto [1992]. The consistency of these four ratios suggests that the Asian emission inventory and DC-8 sampling during TRACE-P were fairly representative of Asian anthropogenic sources.

8. Conclusions

[44] In this paper we present the chemical composition of Asian outflow during the NASA TRACE-P mission in spring 2001. Outflow from the Asian continent had a significant influence on the tropospheric chemical composition over the western Pacific, and this impact extended into the central Pacific. The strongest outflow occurred between 20 and 40°N latitude and at low altitudes. Recent combustion emissions ($\text{C}_2\text{H}_2/\text{CO} \sim 4$) and enhanced species mixing ratios were encountered in the free troposphere and as far east as 150°E longitude reflecting rapid uplift and transport of continental emissions.

[45] Using 5-day backward trajectories, five source regions of continental outflow were identified. These regions were central, coastal, southeast, north-northwest, and west-southwest Asia. Outflow from all five regions was composed of a complex mixture of recent and photochemically aged combustion, industrial, and biomass/biofuel burning emissions. The outflow in each source region contained enhancements in many of the same anthropogenic species. A single pollution source did not dominate any of the air masses sampled from a specific source region. The distance of air mass origin from the western Pacific and the degree of processing in air masses influenced the vertical distribution and magnitude of the species enhancements. These results provide valuable documentation of species mixing ratios and the complexity of Asian continental outflow.

[46] The outflow in each source region contained CO that was at least 3 times larger than background (~ 70 ppbv) and relatively recent emissions as indicated by enhanced hydrocarbon ratios ($\text{C}_2\text{H}_2/\text{CO} \geq 3$ and $\text{C}_3\text{H}_8/\text{C}_2\text{H}_6 \geq 0.2$). As expected, the anthropogenic activity in East Asia had a direct impact on the chemical composition of air masses in the central and coastal regions. The highest mixing ratios for many species and most recent combustion emissions were found in the boundary layer of these two regions. CO, C_2H_2 , CH_3Cl , and C_2Cl_4 were strongly correlated ($r^2 \sim 0.6$ to 0.98) in the central, coastal, and SE regions. Biomass burning was a large source of emissions in SE Asia; however, combustion and industrial sources were also significant. Recent combustion emissions were mixed with processed industrial and biomass/biofuel burning emissions in the NNW region. Aged industrial emissions were also found in the WSW region and were mixed with combustion and biomass burning emissions in the upper troposphere. Convection or lifting associated with mid-latitude cyclones was most likely responsible for the high altitude enhancements observed in the SE and WSW regions. Based on the backward trajectories, the long-range transport of emissions from Africa, the

Middle East, or Europe may have also made a minor contribution to the composition of air masses in the middle and upper troposphere of the NNW and WSW regions.

[47] A comparison between the TRACE-P and PEM-West B missions revealed some important differences. At northern latitudes, O_3 mixing ratios were higher during TRACE-P but were relatively unchanged in southern regions. At low and high altitude, CO was higher during TRACE-P, but it was quite similar in the middle troposphere. C_2H_2 , C_2H_6 , and SO_2 did not exhibit a definite trend between the two missions. C_2Cl_4 was lower at all altitudes during TRACE-P. The $\Delta\text{CO}/\Delta\text{CO}_2$, $\Delta\text{CO}/\Delta\text{CH}_4$, $\Delta\text{C}_2\text{H}_6/\Delta\text{C}_3\text{H}_8$, and $\Delta\text{NO}_y/\Delta(\text{SO}_2 + \text{nss-SO}_4)$ ratios for each source region were compared with the CO/CO_2 , CO/CH_4 , $\text{C}_2\text{H}_6/\text{C}_3\text{H}_8$, and NO_x/SO_2 ratios using data from the 2000 Asian emissions summary. The ratios agreed remarkably well indicating that the measurements obtained during TRACE-P and the emissions inventory were both representative of Asian emissions.

[48] **Acknowledgments.** We would like to thank the NASA Dryden Research Center flight and ground crews for their support during TRACE-P. This research was supported by the NASA Global Tropospheric Chemistry program.

References

- Bachmeier, M. A. S., R. E. Newell, M. C. Shipham, Y. Zhu, D. R. Blake, and E. V. Browell, PEM-West A: Meteorological overview, *J. Geophys. Res.*, *101*, 1655–1677, 1996.
- Berntsen, T. K., S. Karlsdottir, and D. A. Jaffe, Influence of Asian emission on the composition of air reaching the northwestern United States, *Geophys. Res. Lett.*, *26*, 2171–2174, 1999.
- Bey, I., D. J. Jacob, J. A. Logan, and R. M. Yantosca, Asian chemical outflow to the Pacific in spring: Origins, pathways and budgets, *J. Geophys. Res.*, *106*, 23,097–23,113, 2001.
- Blake, D. R., and F. S. Rowland, Urban leakage of liquefied petroleum gas and its impact on Mexico City air quality, *Science*, *269*, 953–956, 1995.
- Blake, D. R., T.-Y. Chen, T. W. Smith Jr., J.-L. C. Wang, O. W. Wingenter, N. J. Blake, and F. S. Rowland, Three-dimensional distribution of non-methane hydrocarbons and halocarbons over the northwestern Pacific during the 1991 Pacific Exploratory Mission (PEM-West A), *J. Geophys. Res.*, *101*, 1763–1778, 1996.
- Blake, N. J., D. R. Blake, T.-Y. Chen, J. E. Collins Jr., G. W. Sachse, B. E. Anderson, and F. S. Rowland, Distribution and seasonality of selected hydrocarbons and halocarbons over the western Pacific basin during PEM-West A and PEM-West B, *J. Geophys. Res.*, *102*, 28,315–28,331, 1997.
- Blake, N. J., et al., NMHCs and halocarbons in Asian continental outflow during TRACE P: Comparison to PEM-West B, *J. Geophys. Res.*, *108*(D20), 8806, doi:10.1029/2002JD003367, in press, 2003.
- Browell, E. V., et al., Large-scale ozone and aerosol distributions, air mass characteristics, and ozone fluxes over the western Pacific Ocean in late-winter/early-spring, *J. Geophys. Res.*, *108*(D20), 8805, doi:10.1029/2002JD003290, in press, 2003.
- Carmichael, G. R., et al., Regional-scale chemical transport modeling in support of intensive field experiments: Overview and analysis of the TRACE-P observations, *J. Geophys. Res.*, *108*(D21), 8823, doi:10.1029/2002JD003117, in press, 2003a.
- Carmichael, G. R., et al., Evaluating regional emission estimates using the TRACE-P observations, *J. Geophys. Res.*, *108*(D21), 8810, doi:10.1029/2002JD003116, in press, 2003b.
- Crutzen, P. J., and M. O. Andreae, Biomass burning in the tropics: Impact on atmospheric chemistry and biogeochemical cycles, *Science*, *250*, 1669–1678, 1990.
- Derwent, R. G., D. R. Middleton, R. A. Field, M. E. Goldstone, J. N. Lester, and R. Perry, Analysis and interpretation of air quality data from an urban roadside location in central London over the period from July 1991 to July 1992, *Atmos. Environ.*, *29*, 923–946, 1995.
- Dibb, J. E., R. W. Talbot, E. Scheuer, G. Seid, M. Avery, and H. Singh, Aerosol chemical composition in Asian continental outflow during TRACE-P: Comparison to PEM-West B, *J. Geophys. Res.*, *108*(D21), 8815, doi:10.1029/2002JD003111, in press, 2003.
- Duce, R. A., C. K. Unni, B. J. Ray, J. M. Prospero, and J. T. Merrill, Long-range atmospheric transport of soil dust from Asia to the tropical North Pacific: Temporal variability, *Science*, *209*, 1522–1524, 1980.

- Fuelberg, H., C. M. Kiley, J. R. Hannan, D. J. Westberg, M. A. Avery, and R. E. Newell, Atmospheric transport during the Transport and Chemical Evolution over the Pacific (TRACE-P) experiment, *J. Geophys. Res.*, 108(D20), 8782, doi:10.1029/2002JD003092, in press, 2003.
- Gregory, G. L., J. T. Merrill, M. C. Shipham, D. R. Blake, G. W. Sachse, and H. B. Singh, Chemical characteristics of tropospheric air over the Pacific Ocean as measured during PEM-West B: Relationship to Asian outflow and trajectory history, *J. Geophys. Res.*, 102, 28,275–28,285, 1997.
- Heald, C. L., D. J. Jacob, P. I. Palmer, M. J. Evans, G. W. Sachse, H. Singh, and D. Blake, Biomass burning emission inventory with daily resolution: Application to aircraft observations of Asian outflow, *J. Geophys. Res.*, 108(D21), 8811, doi:10.1029/2002JD003082, in press, 2003.
- Heikes, B. G., Formaldehyde and hydroperoxides at Mauna Loa Observatory, *J. Geophys. Res.*, 97, 18,001–18,013, 1992.
- Heikes, B., M. Lee, D. Jacob, R. Talbot, J. Bradshaw, H. Singh, D. Blake, B. Anderson, H. Fuelberg, and A. M. Thompson, Ozone, hydroperoxides, oxides of nitrogen, and hydrocarbon budgets in the marine boundary layer over the South Atlantic, *J. Geophys. Res.*, 101, 24,221–24,234, 1996.
- Jacob, D. J., J. A. Logan, and P. P. Murti, Effect of Asian emissions on surface ozone in the United States, *Geophys. Res. Lett.*, 26, 2175–2178, 1999.
- Jacob, D. J., J. H. Crawford, M. M. Kleb, V. E. Connors, R. J. Bendura, J. L. Raper, G. W. Sachse, J. C. Gille, and L. Emmons, The Transport and Chemical Evolution over the Pacific (TRACE-P) mission: Design, execution, and overview of first results, *J. Geophys. Res.*, 108(D20), 8781, doi:10.1029/2002JD003276, in press, 2003.
- Jaffe, D. A., et al., Transport of Asian air pollution to North America, *Geophys. Res. Lett.*, 26, 711–714, 1999.
- Jordan, C. E., B. Anderson, R. W. Talbot, J. E. Dibb, H. E. Fuelberg, C. H. Hudgins, C. M. Kiley, R. Russo, E. Scheuer, G. Seid, K. L. Thornhill, and E. Winstead, Chemical and physical properties of bulk aerosols within four sectors observed during TRACE-P, *J. Geophys. Res.*, 108(D21), 8813, doi:10.1029/2002JD003337, in press, 2003.
- Kang, D., V. P. Aneja, R. G. Zika, C. Farmer, and J. D. Ray, Nonmethane hydrocarbons in the rural southeast United States national parks, *J. Geophys. Res.*, 106, 3133–3155, 2001.
- Kato, N., and H. Akimoto, Anthropogenic emissions of SO₂ and NO_x in Asia: Emission inventories, *Atmos. Environ.*, 26A, 2997–3017, 1992.
- Khalil, M. A. K., R. M. Moore, D. B. Harper, J. M. Lobert, D. J. Erickson, V. Koropalov, W. T. Sturges, and W. C. Keene, Natural emissions of chlorine-containing gases: Reactive Chlorine Emissions Inventory, *J. Geophys. Res.*, 104, 8333–8346, 1999.
- Li, Q., D. J. Jacob, R. M. Yantosca, C. L. Heald, H. Singh, M. Koike, Y. Zhao, G. W. Sachse, and D. G. Streets, A global 3-D model evaluation of the atmospheric budgets of HCN and CH₃CN: Constraints from aircraft measurements over the western Pacific, *J. Geophys. Res.*, 108(D21), 8827, doi:10.1029/2002JD003075, in press, 2003.
- Liu, H., D. J. Jacob, I. Bey, R. M. Yantosca, B. N. Duncan, and G. W. Sachse, Transport pathways for Asian combustion outflow over the Pacific: Interannual and seasonal variations, *J. Geophys. Res.*, 108(D20), 8786, doi:10.1029/2002JD003102, in press, 2003.
- Lobert, J. M., W. C. Keene, J. A. Logan, and R. Yevich, Global chlorine emissions from biomass burning: Reactive Chlorine Emissions Inventory, *J. Geophys. Res.*, 104, 8373–8389, 1999.
- McKeen, S. A., and S. C. Liu, Hydrocarbon ratios and photochemical history of air masses, *Geophys. Res. Lett.*, 20, 2363–2366, 1993.
- Merrill, J. T., M. Uematsu, and R. Black, Meteorological analysis of long range transport of mineral aerosols over the North Pacific, *J. Geophys. Res.*, 94, 8584–8598, 1989.
- Merrill, J. T., R. E. Newell, and A. S. Bachmeier, A meteorological overview for the Pacific Exploratory Mission-West Phase B, *J. Geophys. Res.*, 102, 28,241–28,253, 1997.
- Na, K., Y. P. Kim, and K. C. Moon, Diurnal characteristics of volatile organic compounds in the Seoul atmosphere, *Atmos. Environ.*, 37, 733–742, 2003.
- Novelli, P. C., K. A. Masarie, and P. M. Lang, Distributions and recent changes of carbon monoxide in the lower troposphere, *J. Geophys. Res.*, 103, 19,015–19,033, 1998.
- Rockmann, T., C. A. M. Brenninkmeijer, M. Hahn, and N. F. Elansky, CO mixing and isotope ratios across Russia: Trans-Siberian railroad expedition TROICA 3, April 1997, *Chemosphere Global Change Sci.*, 1, 219–231, 1999.
- Scheeren, H. A., J. Lelieveld, J. A. de Gouw, C. van der Veen, and H. Fischer, Methyl chloride and other chlorocarbons in polluted air during INDOEX, *J. Geophys. Res.*, 107(D19), 8015, doi:10.1029/2001JD001121, 2002.
- Simpson, J. I., N. J. Blake, E. Atlas, F. Flocke, J. H. Crawford, H. E. Fuelberg, C. M. Kiley, F. S. Rowland, and D. R. Blake, Photochemical production and evolution of selected C₂–C₅ alkyl nitrates in tropospheric air influenced by Asian outflow, *J. Geophys. Res.*, 108(D20), 8808, doi:10.1029/2002JD002830, in press, 2003.
- Singh, H. B., and P. B. Zimmerman, Atmospheric distribution and sources of nonmethane hydrocarbons, in *Gaseous Pollutants: Characterization and Cycling*, John Wiley, New York, 1992.
- Singh, H. B., et al., In situ measurements of HCN and CH₃CN in the Pacific troposphere: Sources, sinks, and comparisons with spectroscopic observations, *J. Geophys. Res.*, 108(D20), 8795, doi:10.1029/2002JD003006, in press, 2003.
- Smyth, S., et al., Comparison of free tropospheric western Pacific air mass classification schemes for the PEM-West A experiment, *J. Geophys. Res.*, 101, 1743–1762, 1996.
- Streets, D. G., and S. T. Waldhoff, Biofuel use in Asia and acidifying emissions, *Energy*, 23, 1029–1042, 1998.
- Streets, D. G., and S. T. Waldhoff, Present and future emissions of air pollutants in China: SO₂, NO_x and CO, *Atmos. Environ.*, 34, 363–374, 2000.
- Streets, D. G., et al., An inventory of gaseous and primary aerosol emissions in Asia in the year 2000, *J. Geophys. Res.*, 108(D21), 8809, doi:10.1029/2002JD003093, in press, 2003.
- Talbot, R. W., et al., Chemical characteristics of continental outflow from Asia to the troposphere over the western Pacific Ocean during September–October 1991: Results from PEM-West A, *J. Geophys. Res.*, 101, 1713–1725, 1996a.
- Talbot, R. W., et al., Chemical characteristics of continental outflow over the tropical South Atlantic Ocean from Brazil and Africa., *J. Geophys. Res.*, 101, 24,202–24,287, 1996b.
- Talbot, R. W., et al., Chemical characteristics of continental outflow from Asia to the troposphere over the western Pacific Ocean during February–March 1994: Results from PEM-West B, *J. Geophys. Res.*, 102, 28,255–28,274, 1997.
- Talbot, R., J. Dibb, E. Scheuer, G. Seid, R. Russo, S. Sandholm, D. Tan, H. Singh, D. Blake, N. Blake, E. Atlas, G. Sachse, and M. Avery, Reactive nitrogen in Asian continental outflow over the western Pacific: Results from the NASA TRACE-P airborne mission, *J. Geophys. Res.*, 108(D20), 8803, doi:10.1029/2002JD003129, in press, 2003.
- Tang, Y., et al., The influences of biomass burning during TRACE-P experiment identified by the regional chemical transport model, *J. Geophys. Res.*, 108(D21), 8824, doi:10.1029/2002JD003110, in press, 2003.
- van Aardenne, J. A., G. R. Carmichael, H. Levy II, D. Streets, and L. Hordijk, Anthropogenic NO_x emissions in Asia in the period 1990–2020, *Atmos. Environ.*, 33, 633–646, 1999.
- Vay, S. A., et al., The influence of regional-scale anthropogenic emissions on CO₂ distributions over the western North Pacific, *J. Geophys. Res.*, 108(D20), 8801, doi:10.1029/2002JD003094, in press, 2003.
- Wang, C. J.-L., D. R. Blake, and F. S. Rowland, Seasonal variations in the atmospheric distribution of a reactive chlorine compound, tetrachloroethene (CCL₂ = CCL₂), *Geophys. Res. Lett.*, 22, 1097–1100, 1995.
- Wang, T., A. J. Ding, D. R. Blake, W. Zahorowski, C. N. Poon, and Y. S. Li, Chemical characterization of the boundary layer outflow of air pollution to Hong Kong during February–April 2001, *J. Geophys. Res.*, 2003.
- Yienger, J. J., M. Galanter, T. A. Holloway, M. J. Phadnis, S. K. Guttikunda, G. R. Carmichael, W. J. Moxim, and H. Levy II, The episodic nature of air pollution transport from Asia to North America, *J. Geophys. Res.*, 105, 26,931–26,945, 2000.
- Zahn, A., C. A. M. Brenninkmeijer, W. A. H. Asman, P. J. Crutzen, G. Heinrich, H. Fischer, J. W. M. Cuijpers, and P. F. J. van Velthoven, Budgets of O₃ and CO in the upper troposphere: CARIBIC passenger aircraft results 1997–2001, *J. Geophys. Res.*, 107(D17), 4337, doi:10.1029/2001JD001529, 2002.

E. Atlas and A. Fried, National Center for Atmospheric Research, Boulder, CO 80307, USA. (atlas@ucar.edu; fried@ucar.edu)

M. A. Avery, C. E. Jordan, G. W. Sachse, and S. A. Vay, NASA Langley Research Center, Hampton, VA 23665, USA. (m.a.avery@larc.nasa.gov; c.e.jordan@larc.nasa.gov; g.w.sachse@larc.nasa.gov; s.a.vay@larc.nasa.gov)

D. R. Blake and N. J. Blake, University of California, Irvine, Irvine, CA 92716, USA. (drblake@uci.edu; nblake@uci.edu)

J. E. Dibb, R. S. Russo, E. Scheuer, G. Seid, and R. W. Talbot, University of New Hampshire, Durham, NH 03820, USA. (jack.dibb@unh.edu; russo@resolution.sr.unh.edu; eric.scheuer@unh.edu; garry.seid@unh.edu; robert.talbot@unh.edu)

H. E. Fuelberg, Florida State University, Tallahassee, FL 32306, USA. (fuelberg@met.fsu.edu)

B. G. Heikes and J. Snow, University of Rhode Island, Narragansett, RI 02882, USA. (zagar@notos.gso.uri.edu; snow@gso.uri.edu)

S. T. Sandholm and D. Tan, Georgia Institute of Technology, Atlanta, GA 30332, USA. (scott.sandholm@cas.gatech.edu; tan@easlidar.gtri.gatech.edu)

H. B. Singh, NASA Ames Research Center, Moffett Field, CA 94035, USA. (hsingh@mail.arc.nasa.gov)